LETTER

https://doi.org/10.1038/s41586-019-1285-1

Migrant memory B cells secrete luminal antibody in the vagina

Ji Eun Oh[1,8], Norifumi Iijima[1,6,7,8], Eric Song[1], Peiwen Lu[1], Jonathan Klein[1], Ruoyi Jiang[1], Steven H. Kleinstein[1,2,3] & Akiko Iwasaki[1,4,5]*

Antibodies secreted into mucosal barriers serve to protect the host from a variety of pathogens, and are the basis for successful vaccines[1]. In type I mucosa (such as the intestinal tract), dimeric IgA secreted by local plasma cells is transported through polymeric immunoglobulin receptors[2] and mediates robust protection against viruses[3,4]. However, owing to the paucity of polymeric immunoglobulin receptors and plasma cells, how and whether antibodies are delivered to the type II mucosa represented by the lumen of the lower female reproductive tract remains unclear. Here, using genital herpes infection in mice, we show that primary infection does not establish plasma cells in the lamina propria of the female reproductive tract. Instead, upon secondary challenge with herpes simplex virus 2, circulating memory B cells that enter the female reproductive tract serve as the source of rapid and robust antibody secretion into the lumen of this tract. CD4 tissue-resident memory T cells secrete interferon-γ, which induces expression of chemokines, including CXCL9 and CXCL10. Circulating memory B cells are recruited to the vaginal mucosa in a CXCR3-dependent manner, and secrete virus-specific IgG2b, IgG2c and IgA into the lumen. These results reveal that circulating memory B cells act as a rapidly inducible source of mucosal antibodies in the female reproductive tract.

Antibodies delivered inside the lumen of type II mucosa are capable of blocking infections. In the female reproductive tract (FRT), IgG—but not IgA—are the most protective isotypes against herpes simplex virus 2 (HSV-2) (ref. [5]). When inoculated inside the vaginal cavity, HSV-2-specific IgG confers protection against intravaginal challenge with HSV-2 (refs [6,7]) (Extended Data Fig. 1a). However, the same antibodies injected intravenously had no protective effects[6,7] (Extended Data Fig. 1a), owing to the lack of access of circulating antibodies to the FRT lumen[6,7]. We examined the ability of circulating antibodies (FITC-conjugated IgG) to enter tissues, including the FRT lumen. FITC–IgG was detected in the spleen and lung two hours after intravenous injection, whereas it was barely detectable in the vaginal parenchyma or mucosa even after 24-h post-injection (Extended Data Fig. 1b). This is consistent with the fact that levels of antigen-specific IgG in the cervicovaginal secretions of women immunized with human papillomavirus vaccine[8], influenza vaccine[9] and tetanus toxoid[10] are less than 1–0.1% of those found in circulation.

For viruses such as the human papillomavirus, which requires breach of the epithelial barrier and minor abrasion for infection, serum antibodies can access the site of infection to confer protection[11]. We tested whether serum antibodies enter the vaginal lumen in response to a minor breach in the barrier. In intact mice, virus-specific antibody was not detected in the vaginal lumen of mice immunized subcutaneously with an attenuated thymidine-kinase mutant (TK^-) HSV-2 (Extended Data Fig. 1c), despite the presence of serum antibodies (Extended Data Fig. 1d). However, virus-specific antibody was detected in the vaginal lumen (Extended Data Fig. 1c) after epithelial barrier breach with a cervical brush (Extended Data Fig. 1e). Thus, at steady state, circulating antibodies do not access the vaginal lumen.

Systemic inoculation of live attenuated simian immunodeficiency virus establishes plasma cells in the FRT[12]. Whether vaginal IgG secretion can be enhanced by other means of immunization remains unclear, and is a key question in the field of vaccines against sexually transmitted infections. To address this question, we first examined the presence of B cells within the FRT following intravaginal immunization with TK^- HSV-2. No increase in the percentage or the number of plasmablasts ($CD138^+CD19^+$), plasma cells ($CD138^+CD19^-$) or $CD138^-CD19^+$ B cells was detected in the vagina five weeks after immunization (Fig. 1a). The B-cell number remained low in the vagina, even after inducing local inflammation with intravaginal inoculation with CpG five days after priming with TK^- HSV-2 (Extended Data Fig. 2a). Analysis of vaginal tissue sections showed very few $B220^+$ cells in naive or immunized mice. We detected rare $CD138^+B220^-$ plasmablast and plasma cells scattered throughout the vaginal lamina propria after immunization (Fig. 1b), consistent with a previous study[13]. Nevertheless, the presence of B cells or plasma cells paled in comparison to the robust formation of the CD4 T cells within the memory lymphocyte cluster[14] (Fig. 1b). We also examined the presence of B cells within the upper FRT. Similar to the vaginal mucosa, no increase in the number of plasmablasts, plasma cells or $CD138^-CD19^+$ B cells was observed in the cervix and uterus five weeks after immunization (immune group, Extended Data Fig. 3).

Next, we examined the levels of secreted HSV-2-specific antibodies in the vaginal lumen and in circulation five weeks after immunization (Extended Data Fig. 1f, g). Intranasal immunization with the influenza virus A strain PR8 was included as a reference. In broncho-alveolar lavage fluid, high levels of flu-specific antibodies were detected even after five weeks of immunization (Extended Data Fig. 1f). By contrast, vaginal secretions contained low levels of HSV-2-specific antibodies, despite the high levels of circulating antibodies (Extended Data Fig. 1f, g). Antibody levels in the vaginal lumen were not substantially enhanced by local inflammation induced by intravaginal inoculation with CpG five days after immunization (Extended Data Fig. 2b, c). These results indicated that—unlike in the respiratory mucosa—a very limited amount of circulating antibodies enter the vaginal lumen after immunization.

Next, we investigated luminal antibody secretion after secondary challenge with vaginal wild-type HSV-2, in mice that were previously vaginally immunized with TK^- HSV-2 (Fig. 1c). Notably, virus-specific IgG2b, IgG2c, IgG1 and IgA were rapidly secreted into the vaginal lumen, as early as one-day post-challenge. Naive mice that were intravaginally challenged for the first time with HSV-2 had no detectable virus-specific antibodies in the time frame that we examined (Fig. 1c). After secondary viral challenge, a rapid and robust recruitment of IgG^+ B cells to the vagina was observed (Fig. 1d). An increased number of plasma cells in the cervix and uterus was also observed soon

[1]Department of Immunobiology, Yale School of Medicine, New Haven, CT, USA. [2]Department of Pathology, Yale School of Medicine, New Haven, CT, USA. [3]Interdepartmental Program in Computational Biology and Bioinformatics, Yale University, New Haven, CT, USA. [4]Department of Molecular Cellular and Developmental Biology, Yale University, New Haven, CT, USA. [5]Howard Hughes Medical Institute, Chevy Chase, MD, USA. [6]Present address: Laboratory of Adjuvant Innovation, National Institutes of Biomedical Innovation, Health and Nutrition, Ibaraki City, Japan. [7]Present address: Immunology Frontier Research Center, Osaka University, Ibaraki City, Japan. [8]These authors contributed equally: Ji Eun Oh, Norifumi Iijima. *e-mail: akiko.iwasaki@yale.edu

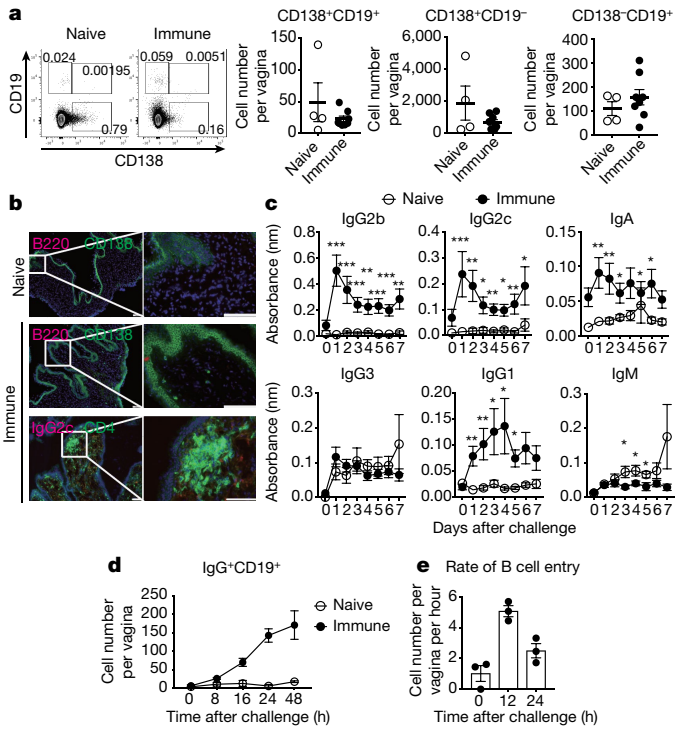

Fig. 1 | Memory B cells rapidly migrate into the FRT upon secondary challenge in immunized mice. a, **b**, C57BL/6 mice were intravaginally immunized with TK$^-$ HSV-2 (immune). **a**, Five weeks later, CD138$^+$CD19$^+$, CD138$^+$CD19$^-$ and CD138$^-$CD19$^+$ cells in vaginal tissues were analysed in both naive ($n = 4$) and immunized ($n = 8$) mice by flow cytometry. **b**, Six weeks later, frozen sections of vagina were stained with antibodies against CD138 and CD4 (green), B220 and IgG2c (red), and DAPI (blue). Scale bars, 100 μm. **c**, **d**, C57BL/6 mice, with or without immunization with TK$^-$ HSV-2 five weeks prior, were intravaginally challenged with wild-type (WT) HSV-2. **c**, Following the indicated days after challenge, HSV-2-specific antibodies in vaginal wash were measured by enzyme-linked immunosorbent assay (ELISA) (naive, $n = 9$ mice; immune, $n = 13$ mice). Sample dilution was 1:7. **d**, After challenge, the number of B cells in the vagina was analysed by flow cytometry (naive, $n = 3$ mice; immune, $n = 4$ mice). **e**, B cells isolated from DsRed mice immunized with TK$^-$ HSV-2 five weeks prior were adoptively transferred into mice immunized with TK$^-$ HSV-2 five weeks prior, at the indicated hours after secondary challenge with wild-type HSV-2. Vaginal tissues were collected two hours after adoptive transfer, and the number of DsRed$^+$IgG$^+$ B cells in vaginal tissues was analysed by flow cytometry ($n = 3$ mice). Data are mean ± s.e.m. Data are pooled from two (**a**) and four (**c**) independent experiments, or are representative of three (**b**, **d**) and two (**e**) independent experiments. *$P < 0.05$, **$P < 0.01$, ***$P < 0.001$ (two-tailed Mann–Whitney U test).

after secondary challenge (Extended Data Fig. 3). These results are consistent with the recruitment of B cells that has previously been observed after restimulation of CD4 tissue-resident memory T cells (T_{RM} cells) or CD8 T_{RM} cells in the FRT[15,16]. Primary infection of naive mice with HSV-2 resulted in a minimal increase in B-cell migration within the first 48 h (Fig. 1d), which indicates that the immune status of the host was required for this rapid B-cell migration into the FRT. Memory B cells can be categorized into CD80$^+$PD-L2$^+$ cells, which differentiate rapidly into antibody-forming cells, and CD80$^-$PD-L2$^-$ memory B cells that generate few early antibody-forming cells, but which robustly seed germinal centres[17]. Notably, about half of IgD$^-$IgG$^+$ B cells (memory B cells) in the FRT of secondarily challenged mice expressed both CD80 and PD-L2 (Extended Data Fig. 4a), and these CD80$^+$PD-L2$^+$ memory B cells accumulated in the FRT (Extended Data Fig. 4b). To measure the rate of B-cell entry into the vagina after secondary challenge, B cells from DsRed-transgenic immune animals were adoptively transferred to host mice that were previously immunized with TK$^-$ HSV-2. The entry of transferred B cells peaked at 12 h after re-challenge, and remained high at 24 h (Fig. 1e). An increased proportion of IgG$^+$ B cells that are recruited to the vaginal tissue in response to secondary challenge with HSV-2 expressed the costimulatory molecule CD86 as well as the activation marker CD69 (Extended Data Fig. 5a). Further analysis demonstrated that VCAM-1 expression on endothelial cells in lamina propria rapidly increased after HSV-2 challenge (Extended Data Fig. 5b), consistent with a previous study[18], possibly providing an adhesion molecule for the recruitment of B cells to the vaginal mucosa. Long-term tracking of B cells in the vagina showed a peak accumulation at around five days after re-challenge, followed by a decline over several weeks (Extended Data Fig. 5c). In contrast to mice immunized vaginally, mice immunized through subcutaneous injection with TK$^-$ HSV-2 did not show B-cell recruitment into the FRT upon vaginal challenge with wild-type HSV-2 (Extended Data Fig. 6a), despite the fact that the two routes of immunization (subcutaneous and intravaginal) led to similar levels of circulating antibody (Extended Data Fig. 6b). Thus, in mice immunized locally with TK$^-$ HSV-2, IgG$^+$ B cells are recruited rapidly to the vagina shortly after secondary challenge and become activated in the tissue. These cells remain within the vaginal tissue for several weeks after the secondary challenge.

We next investigated whether antigen-specific, active virus challenge is necessary for the recruitment of B cells to the FRT. Intravaginal challenge with a heterologous virus (influenza A strain PR8) or stimulation with CpG1826 to induce inflammation in the FRT[19] failed to recruit B cells into the vagina of immunized mice (Extended Data Fig. 7a–c). By contrast, vaginal inoculation of heat-inactivated wild-type HSV-2 induced considerable recruitment of B cells into the tissue, with an accompanying increase in the luminal secretion of HSV-2-specific antibodies (Extended Data Fig. 7d, e). These data indicated that a local antigen-specific recall response is required for the recruitment of IgG$^+$ B cells and secretion of antigen-specific IgG.

To determine whether B-cell migration is required for local antibody secretion, we examined the secretion of virus-specific immunoglobulin in the vaginal wash after treatment with FTY720 (an agonist of S1PR1)[20]. This treatment resulted in a large reduction in the number of B cells in the FRT (Fig. 2a), and had no effects on resident dendritic cell population (Fig. 2a) or T_{RM} cell population[14]. Notably, intravaginal challenge with HSV-2 of FTY720-treated immune mice resulted in a severe reduction in the levels of IgG2b, IgG2c and IgA that were secreted into the vaginal lumen (Fig. 2b). FTY720 treatment did not affect serum levels of antiviral immunoglobulin (Extended Data Fig. 8), as most of the serum antibodies are secreted by stationary plasma cells in the bone marrow[21]. These data indicated that the migration of B cells to the FRT is a prerequisite for the local secretion of IgG2b, IgG2c and IgA.

To probe the nature of IgG$^+$ B cells recruited into the FRT after secondary challenge with HSV-2, we collected vagina-infiltrating lymphocytes for single-cell RNA sequencing (scRNA-seq) analysis. We also included a control group of mice that received a primary vaginal infection with wild-type HSV-2 one day before lymphocytes were collected. Compared to the primary-infected mice, the FRT of previously immunized mice after secondary challenge contained a larger population of CD4 and CD8 T cells with a tissue-resident phenotype (Extended Data Fig. 9a), consistent with previous findings[14]. A focused clustering of CD19 B cells was performed to identify subtypes of B cell (Extended Data Fig. 9b). B cells that infiltrated the FRT after immunization belonged to a greater diversity of clusters than those in the primary-infected FRT (seven versus three populations) (Extended Data Fig. 9c). These cells in the FRT of secondary infected mice included cells that resembled follicle-associated B cells, plasma cells and memory B cells, which expressed genes such as *Sdc1* (also known as *Cd138*), *Ighg2b* and *Il9r*[22,23] (Extended Data Fig. 9c, d). Expression of the chemokine receptors *Cxcr3* and *Ccr6* localized to populations that resembled memory, light-zone and dark-zone B-cell populations, and showed high expression of the activation markers *Cd86*, *Cd80* and *Cd69* (Extended Data Fig. 9d). To further elucidate

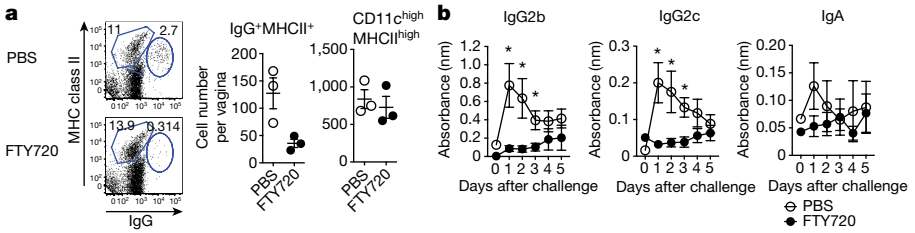

Fig. 2 | Rapid B-cell recruitment into the FRT upon secondary challenge is a prerequisite for antibody secretion into the vaginal lumen. a, **b**, C57BL/6 mice were infected vaginally with TK$^-$ HSV-2 five weeks previously. Mice were given drinking water containing 4 μg ml^{-1} of FTY720 for two weeks. **a**, One day after secondary challenge, the number of IgG$^+$MHC class II$^+$ cells and CD11c^{high}MHC class II^{high} cells were analysed by flow cytometry ($n = 3$ mice). **b**, After challenge, HSV-2-specific antibodies in vaginal wash were measured by ELISA ($n = 5$ mice). Sample dilution for ELISA was 1:7. Data are mean ± s.e.m. Data are representative of two (**a**) independent experiments, or are pooled from two (**b**) independent experiments. *$P < 0.05$ (two-tailed Mann–Whitney U test).

differences between the B cells that infiltrate the FRT after primary and secondary infection, we focused on FRT-associated B cells and identified five distinct populations, including one that was unique to immunized mice (cluster 4) (Extended Data Fig. 9e). This cluster-4 population expressed *Ighg2b*, *Cd69*, *Lax1* (a negative regulator of B-cell receptor (BCR), which is expressed by activated B cells[24]) and *Cxcr3* (Extended Data Fig. 9f). Furthermore, the FRT of mice that experienced the secondary challenge lost cluster 3, and instead gained three other populations (clusters 0, 1 and 2), and showed enrichment of genes such as *Nr4a1* (which encodes NUR77, a marker of surface BCR engagement[25]), *Il21r*, *Cd69* and IFNγ-stimulated genes (Extended Data Fig. 9f).

To test whether B-cell clones in the FRT after re-challenge are clonally related to the spleen, B cells were sorted from the spleen and clonal assignments were made using Change-O[26] (see Methods). We identified a significant difference in the number of clones that spanned both compartments during secondary and primary infection (Extended Data Fig. 9g). One clone (clone IGHV5-17 IGHJ4/45) represented the largest clone that was present in the spleen (Extended Data Fig. 9h). Moreover, the splenic relative and vaginal descendants had gene-expression profiles that were consistent with plasma cells and IgG production (Extended Data Fig. 9h).

To determine the migration cues that are responsible for recruiting circulating memory B cells after secondary viral challenge, we examined chemokine receptors expressed on memory B cells in the blood. Five weeks after immunization, a subset of IgG$^+$CD19$^+$IgD$^-$ memory B cells in circulation expressed the CCR6, CXCR3 and CXCR5

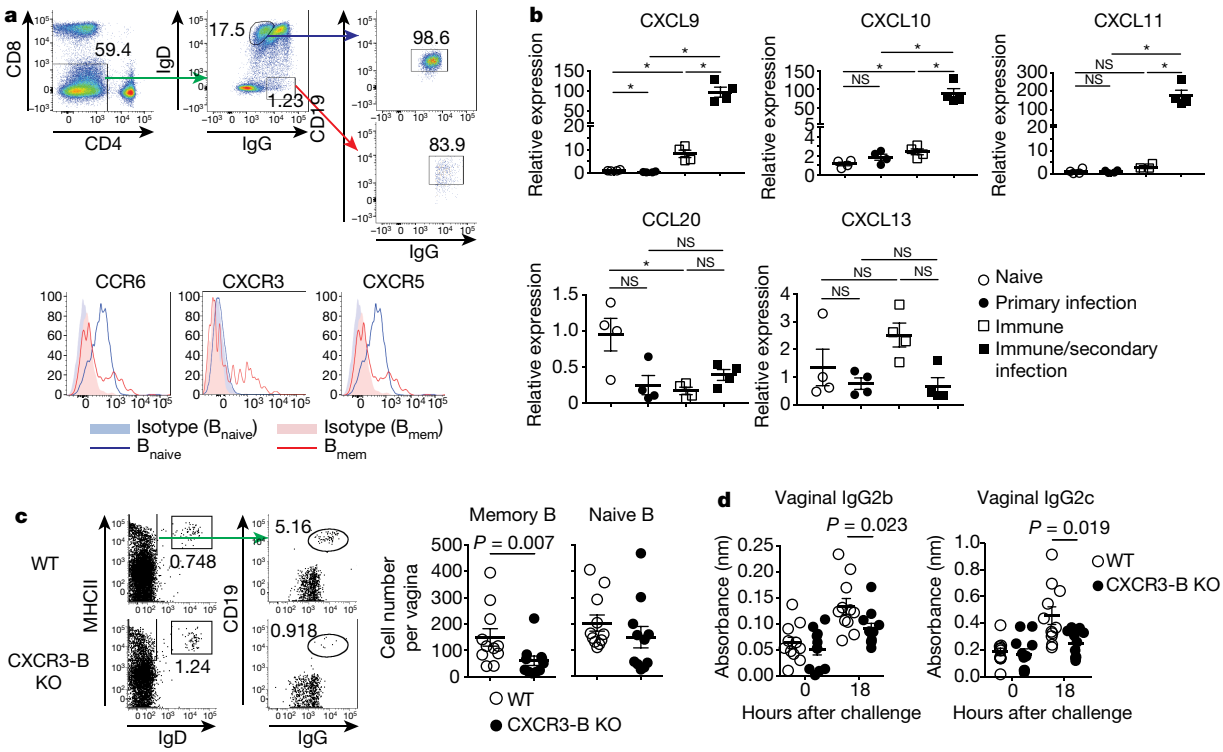

Fig. 3 | CXCR3 is indispensable for the recruitment of memory B cells into the vagina upon secondary challenge with HSV-2. a, C57BL/6 mice were immunized intravaginally with TK$^-$ HSV-2. Five weeks later, the expression of various chemokine receptors on circulating IgD$^-$IgG$^+$ memory B cells (B_{mem}) or IgD$^+$IgG$^-$ naive B (B_{naive}) cells in the blood was analysed by flow cytometry. **b**, Eight hours after challenge in naive or TK$^-$ HSV-2-immunized mice, the mRNA expression of various chemokines (relative to naive mice) was measured in vaginal tissues by real-time quantitative PCR ($n = 4$ mice). *$P = 0.029$, Wilcoxon rank-sum test. **c**, **d**, Mixed bone-marrow chimeric mice that lacked CXCR3 only on B cells (CXCR3-B KO) were immunized intravaginally with TK$^-$ HSV-2. Five weeks later, mice were challenged with wild-type HSV-2. **c**, Eighteen hours after challenge, the number of IgD$^+$ naive B cells and IgG$^+$ memory B cells in vaginal tissues was analysed by flow cytometry ($n = 11$ mice). KO, knockout. **d**, Eighteen hours after challenge, HSV-2-specific antibodies in vaginal wash were measured by ELISA ($n = 11$ mice). Sample dilution for ELISA was 1:10. Data are mean ± s.e.m. Data are representative of four (**a**) and two (**b**) independent experiments, or are pooled from two independent experiments (**c**, **d**). NS, non-significant (two-tailed Mann–Whitney U test).

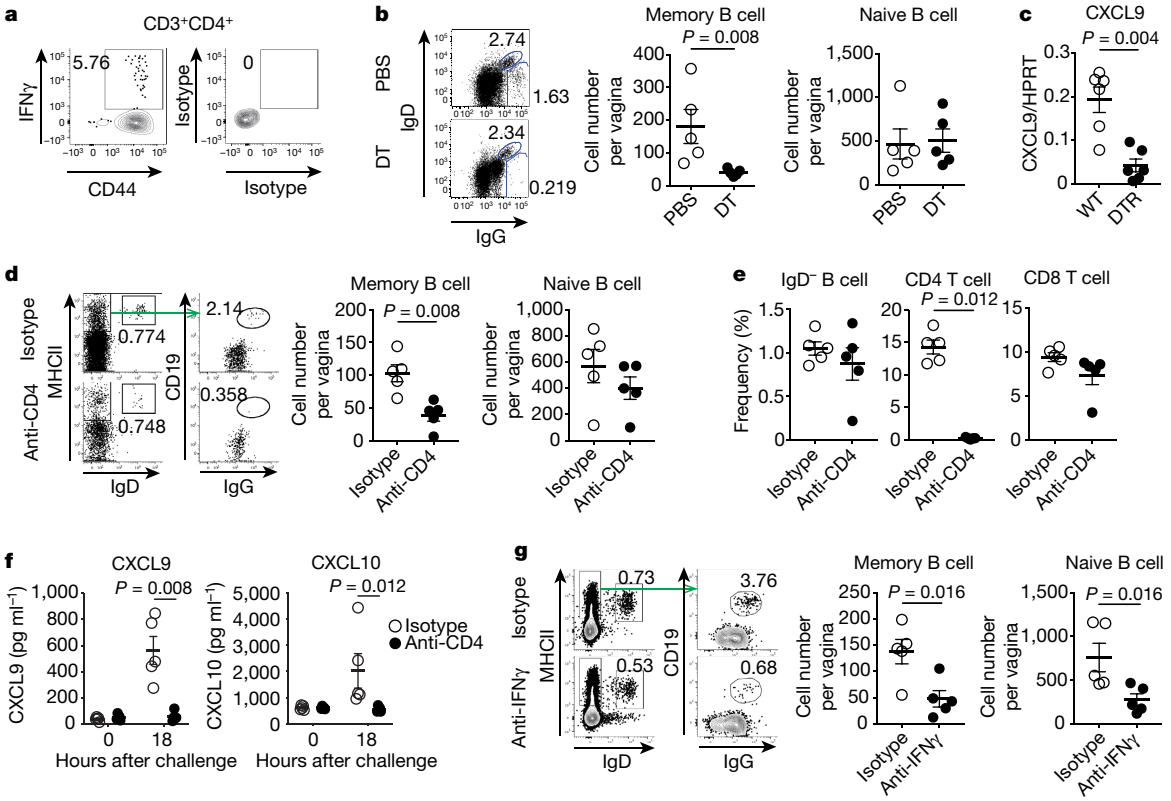

Fig. 4 | CD4 T_{RM} cells have an essential role in the recruitment of memory B cells upon secondary challenge in immunized mice. **a**, C57BL/6 mice were immunized intravaginally with TK$^-$ HSV-2. Five weeks later, HSV-2-specific IFNγ$^+$CD44$^+$CD4$^+$ T cells in the vagina were analysed by flow cytometry. **b**, **c**, CD11b–DTR (CD11b-promoter driven diphtheria toxin receptor) bone-marrow chimeric mice were immunized intravaginally with TK$^-$ HSV-2. **b**, Eight weeks later, these mice were treated with diphtheria toxin (DT) to deplete CD11b$^+$ macrophages, and challenged with wild-type HSV-2. One day later, the number of IgD$^+$ naive B cells and IgG$^+$ memory B cells in vaginal tissues was analysed by flow cytometry ($n = 5$ mice). **c**, Five weeks after immunization, diphtheria-toxin-treated chimeric mice were challenged with wild-type HSV-2. Eight hours later, mRNA expression of *Cxcl9* in vaginal tissue was measured by real-time quantitative PCR ($n = 6$ mice). **d**–**f**, C57BL/6 mice were immunized intravaginally with TK$^-$ HSV-2. Five weeks later, mice were treated with anti-CD4 antibody to deplete CD4 T cells. **d**, One day after challenge with wild-type HSV-2, the number of IgD$^+$ naive B cells and IgG$^+$ memory B cells in vaginal tissues was analysed by flow cytometry ($n = 5$ mice). **e**, The frequency of circulating memory B cells, CD4 T cells and CD8 T cells in blood after CD4 depletion were analysed by flow cytometry ($n = 5$ mice). **f**, Eighteen hours after challenge, the level of CXCL9 and CXCL10 chemokines in vaginal wash was measured by ELISA ($n = 5$ mice). **g**, C57BL/6 mice immunized intravaginally with TK$^-$ HSV-2 were treated with anti-IFNγ antibody. One day after challenge with wild-type HSV-2, the number of IgD$^+$ naive B cells and IgG$^+$ memory B cells in vaginal tissues was analysed by flow cytometry ($n = 5$ mice). Data are mean ± s.e.m. (two-tailed Mann–Whitney *U* test). Data are representative of two (**a**–**c**, **g**) and three (**d**–**f**) independent experiments.

chemokine receptors (Fig. 3a), consistent with our scRNA-seq results (Extended Data Fig. 9d–f), but not other chemokine receptors (Extended Data Fig. 10a). By contrast, naive B cells (IgG$^-$CD19$^+$IgD$^+$) did not express CXCR3 (Fig. 3a). Analysis of vaginal chemokine expression eight hours after secondary challenge showed that *Cxcl9*, *Cxcl10* and *Cxcl11* (the CXCR3 ligand) were highly expressed and that *Ccl20* (the CCR6 ligand) and *Cxcl13* (the CXCR5 ligand) were not (Fig. 3b). The proportion of CXCR3-expressing memory B cells in circulation in secondarily challenged mice was high compared to those in circulation after primary infection (Extended Data Fig. 10b). After primary infection, mice also showed a delayed expression of the CXCR3 ligand CXCL9 in the vagina, compared to the expression in secondarily challenged immunized mice (Extended Data Fig. 10c), which provides a possible explanation for why the primary infection did not elicit B-cell recruitment in the FRT lumen (Fig. 1d). To examine whether CXCR3 expression on B cells is required for recruitment to the FRT, we generated mixed bone-marrow chimeric mice that lack CXCR3 only on B lymphocytes (Extended Data Fig. 10d). We confirmed that CXCR3 was deficient only on B cells, and not on T cells, in these chimeric mice (Extended Data Fig. 10e). CXCR3 ablation on B cells did not affect the number of circulating memory B cells and T cells in the blood (Extended Data Fig. 10f). However, the chimeric mice showed a reduction in the number of memory B cells that entered into the vagina, whereas the number of naive B cells that was detected in the vagina after secondary intravaginal challenge with HSV-2 was comparable between the wild-type and chimeric mice (Fig. 3c). Moreover, the secretion of the virus-specific antibodies IgG2b and IgG2c was also impaired in chimeric mice that lack CXCR3 only on B cells after secondary challenge with HSV-2 (Fig. 3d). Taken together, these results indicated that CXCR3 is required for the recruitment of circulating memory B cells, as well as their subsequent secretion of antibodies into the vaginal cavity after secondary challenge.

Our data showed that immune, but not naive, mice are competent for memory B-cell recruitment into the FRT (Fig. 1d). Thus, we next focused on the role of the memory lymphocyte cluster and CD4 T_{RM} cells in recruitment of memory B cells in the vagina. CXCR3 ligands are interferon (IFN)-inducible chemokines, and CD4 T cells in the vagina are important source of IFNγ production[27] (Fig. 4a). CD4 T_{RM} cells in the vagina of immunized mice are maintained in memory lymphocyte clusters by a local network of macrophages; the depletion of CD11b$^+$ cells in mice that were previously immunized intravaginally with TK$^-$ HSV-2 results in a loss of cells of the memory lymphocyte cluster, as well as the disappearance of the cluster structure[14]. Depletion of CD11b$^+$ cells resulted in the block of memory B-cell, but not naive B-cell, recruitment after secondary challenge (Fig. 4b). In addition, *Cxcl9* expression in the vagina after secondary challenge in immunized mice was defective after depletion of CD11b$^+$ cells (Fig. 4c). Depletion of CD4 T cells in immunized mice showed a reduction in the number

of memory B cells, but not of naive B cells, in the vagina after secondary challenge (Fig. 4d), without affecting the number of circulating memory B cells (Fig. 4e). Moreover, the production of CXCR3 ligands in the vagina was impaired in CD4-T-cell-depleted mice upon secondary challenge (Fig. 4f). In addition, neutralization of IFNγ in immunized mice impaired the recruitment of B cells into the vagina after secondary challenge with HSV-2 (Fig. 4g). These results indicated that CD4 T_{RM} cells maintained by the macrophages in memory lymphocyte clusters have a critical role in recruiting circulating memory B cells into the vagina after secondary challenge, by secreting IFNγ (which induces CXCL9 and CXCL10).

Antibody secretion into the FRT is an inefficient process at the steady state, in part owing to the lack of tissue-resident plasma cells. Our results show that local immunization with an attenuated HSV-2 strain induces a microenvironment that is conducive to the rapid and robust recruitment of circulating memory B cells upon secondary challenge; these memory B cells secrete high levels of virus-specific antibodies into the vaginal lumen.

Antibody-based vaccines against HSV-2 have failed to confer protection in humans[28]. None of these vaccines has achieved the supraphysiological levels of antibodies that are needed within the vaginal lumen to protect the host from HSV-2 (ref. [11]). Our study has shown that a high level of anti-viral antibodies in blood does not translate into antibody presence in the vaginal lumen. Thus, despite the presence of the neonatal crystallisable fragment (Fc) receptor, circulating antibodies fail to enter the vaginal lumen and thus there is little protective effect in the vagina. For pathogens—including HSV-1 or HSV-2—that do not require compromised barriers for infection, high existing titres of luminal antiviral antibodies are key to conferring protection. Our current results reveal an inducible means of providing robust antibody secretion into the FRT. This understanding may be leveraged to create robust antibody-mediated vaccines against sexually transmitted infections.

Online content

Any methods, additional references, Nature Research reporting summaries, source data, extended data, supplementary information, acknowledgements, peer review information; details of author contributions and competing interests; and statements of data and code availability are available at https://doi.org/10.1038/s41586-019-1285-1.

Received: 19 June 2018; Accepted: 14 May 2019;
Published online 12 June 2019.

1. Plotkin, S. A. Correlates of protection induced by vaccination. *Clin. Vaccine Immunol.* **17**, 1055–1065 (2010).
2. Iwasaki, A. Mucosal dendritic cells. *Annu. Rev. Immunol.* **25**, 381–418 (2007).
3. Franco, M. A., Angel, J. & Greenberg, H. B. Immunity and correlates of protection for rotavirus vaccines. *Vaccine* **24**, 2718–2731 (2006).
4. Patel, M. et al. A systematic review of anti-rotavirus serum IgA antibody titer as a potential correlate of rotavirus vaccine efficacy. *J. Infect. Dis.* **208**, 284–294 (2013).
5. Parr, E. L. & Parr, M. B. Immunoglobulin G is the main protective antibody in mouse vaginal secretions after vaginal immunization with attenuated herpes simplex virus type 2. *J. Virol.* **71**, 8109–8115 (1997).
6. Whaley, K. J., Zeitlin, L., Barratt, R. A., Hoen, T. E. & Cone, R. A. Passive immunization of the vagina protects mice against vaginal transmission of genital herpes infections. *J. Infect. Dis.* **169**, 647–649 (1994).
7. Sherwood, J. K., Zeitlin, L., Whaley, K. J., Cone, R. A. & Saltzman, M. Controlled release of antibodies for long-term topical passive immunoprotection of female mice against genital herpes. *Nat. Biotechnol.* **14**, 468–471 (1996).
8. Nardelli-Haefliger, D. et al. Specific antibody levels at the cervix during the menstrual cycle of women vaccinated with human papillomavirus 16 virus-like particles. *J. Natl Cancer Inst.* **95**, 1128–1137 (2003).
9. Crowley-Nowick, P. A. et al. Rectal immunization for induction of specific antibody in the genital tract of women. *J. Clin. Immunol.* **17**, 370–379 (1997).
10. Bouvet, J. P., Bélec, L., Pirès, R. & Pillot, J. Immunoglobulin G antibodies in human vaginal secretions after parenteral vaccination. *Infect. Immun.* **62**, 3957–3961 (1994).
11. Iwasaki, A. Exploiting mucosal immunity for antiviral vaccines. *Annu. Rev. Immunol.* **34**, 575–608 (2016).
12. Li, Q. et al. Live simian immunodeficiency virus vaccine correlate of protection: local antibody production and concentration on the path of virus entry. *J. Immunol.* **193**, 3113–3125 (2014).
13. Parr, E. L. & Parr, M. B. Immunoglobulin G, plasma cells, and lymphocytes in the murine vagina after vaginal or parenteral immunization with attenuated herpes simplex virus type 2. *J. Virol.* **72**, 5137–5145 (1998).
14. Iijima, N. & Iwasaki, A. A local macrophage chemokine network sustains protective tissue-resident memory CD4 T cells. *Science* **346**, 93–98 (2014).
15. Beura, L. K. et al. $CD4^+$ resident memory T cells dominate immunosurveillance and orchestrate local recall responses. *J. Exp. Med.* **216**, 1214–1229 (2019).
16. Schenkel, J. M. et al. Resident memory CD8 T cells trigger protective innate and adaptive immune responses. *Science* **346**, 98–101 (2014).
17. Zuccarino-Catania, G. V. et al. CD80 and PD-L2 define functionally distinct memory B cell subsets that are independent of antibody isotype. *Nat. Immunol.* **15**, 631–637 (2014).
18. Parr, M. B. & Parr, E. L. Interferon-γ up-regulates intercellular adhesion molecule-1 and vascular cell adhesion molecule-1 and recruits lymphocytes into the vagina of immune mice challenged with herpes simplex virus-2. *Immunology* **99**, 540–545 (2000).
19. Gill, N., Deacon, P. M., Lichty, B., Mossman, K. L. & Ashkar, A. A. Induction of innate immunity against herpes simplex virus type 2 infection via local delivery of Toll-like receptor ligands correlates with beta interferon production. *J. Virol.* **80**, 9943–9950 (2006).
20. Matloubian, M. et al. Lymphocyte egress from thymus and peripheral lymphoid organs is dependent on S1P receptor 1. *Nature* **427**, 355–360 (2004).
21. Benner, R., Hijmans, W. & Haaijman, J. J. The bone marrow: the major source of serum immunoglobulins, but still a neglected site of antibody formation. *Clin. Exp. Immunol.* **46**, 1–8 (1981).
22. Takatsuka, S. et al. IL-9 receptor signaling in memory B cells regulates humoral recall responses. *Nat. Immunol.* **19**, 1025–1034 (2018).
23. Wang, Y. et al. Germinal-center development of memory B cells driven by IL-9 from follicular helper T cells. *Nat. Immunol.* **18**, 921–930 (2017).
24. Zhu, M. et al. Negative regulation of lymphocyte activation by the adaptor protein LAX. *J. Immunol.* **174**, 5612–5619 (2005).
25. Mueller, J., Matloubian, M. & Zikherman, J. Cutting edge: An in vivo reporter reveals active B cell receptor signaling in the germinal center. *J. Immunol.* **194**, 2993–2997 (2015).
26. Gupta, N. T. et al. Hierarchical clustering can identify B cell clones with high confidence in Ig repertoire sequencing data. *J. Immunol.* **198**, 2489–2499 (2017).
27. Iwasaki, A. The role of dendritic cells in immune responses against vaginal infection by herpes simplex virus type 2. *Microbes Infect.* **5**, 1221–1230 (2003).
28. Awasthi, S. & Friedman, H. M. Status of prophylactic and therapeutic genital herpes vaccines. *Curr. Opin. Virol.* **6**, 6–12 (2014).

Publisher's note: Springer Nature remains neutral with regard to jurisdictional claims in published maps and institutional affiliations.

© The Author(s), under exclusive licence to Springer Nature Limited 2019

METHODS

No statistical methods were used to predetermine sample size. The experiments were not randomized and investigators were not blinded to allocation during experiments and outcome assessment.

Mice. Six-to-eight-week-old female C57BL/6 (CD45.2$^+$), congenic C57BL/6 B6.SJL-PtprcaPep3b/BoyJ (B6.Ly5.1) (CD45.1$^+$), B6.129S2-*Igh*^{tm1Cgn}/J (μMT), B6.FVB-Tg (ITGAM-DTR/EGFP) 34Lan/J (CD11bDTR), B6.Cg-Tg(CAG-DsRed*MST)1Nagy/J (DsRed), and B6.129P2-*Cxcr3*^{tm1Dgen}/J (*Cxcr3*$^{-/-}$) mice were purchased from the National Cancer Institute and Jackson Laboratory. All procedures used in this study complied with federal guidelines and institutional policies by the Yale animal care and use committee.

Viruses. HSV-2 strains 186syn$^-$ TK$^-$ and 186syn$^+$ were generous gifts from D. Knipe (Harvard Medical School). These viruses were propagated and titrated on Vero cells (ATCC CCL-81) as previously described[29] (Vero cells were negative for mycoplasma contamination). Influenza virus strain A/Puerto Rico/8/34 (H1N1) was a gift from P. Staeheli (University Medical Center Freiburg). Influenza virus strain A/PR/8/34 (H1N1) was propagated as previously described[30].

Virus infection. Six-to-eight-week-old female mice were injected subcutaneoulsy with Depo Provera (Pharmacia Upjohn) at 2 mg per mouse in 100 μl at 5–7 d before infection, swabbed with calcium alginate and inoculated intravaginally with 10^5 plaque-forming units (pfu) of HSV-2 (186syn$^-$ TK$^-$) or 2,500 pfu of wild-type HSV-2 (186syn$^+$) in 10 μl using a blunt-ended micropipette tip as previously described[31]. In some experiments, mice were inoculated subcutaneously with 10^6 pfu of TK$^-$ HSV-2 in 100 μl. For secondary challenge, immunized mice were challenged vaginally with 10^4–10^5 pfu of wild-type HSV-2 (186syn$^+$) (100% lethal dose for naive mice). The severity of disease was scored as: 0, no sign; 1, slight genital erythema and oedema; 2, moderate genital inflammation; 3, purulent genital lesions; 4, hindlimb paralysis; 5, premoribund. Owing to humane concerns, the animals were euthanized before reaching a moribund state[29]. For boosting with inactive virus, immunized mice were injected intravaginally with 10^5 pfu of heat-inactivated wild-type HSV-2. For influenza A virus infection, mice were anaesthetized by intraperitoneal injection of ketamine and xylazine, and inoculated intranasally with 10–20 pfu of a highly virulent variant of A/PR8/34 (H1N1) in 20 μl PBS as previously described[30].

Vaginal viral titres. Vaginal fluids were collected on days 1–5 after infection, using calcium alginate swabs and PBS. To measure virus titre, vaginal washes were collected in ABC buffer (0.5 mM $MgCl_26H_2O$, 0.9 mM $CaCl_22H_2O$, 1% glucose, 5% HI FBS and penicillin–streptomycin). Viral titres were obtained by titration of vaginal wash samples on Vero cell monolayer as previously described[29].

Antibodies. Anti-CD45.2 (104), anti-CD45.1 (A20), anti-CD45 (30-F11), anti-CD3ε (145-2C11), anti-CD4 (GK1.5 and RM4-5), anti-CD8α (53-6.7), anti-CD19 (6D5 and 1D3), anti-CD45R/B220 (RA3-6B2), anti-CD138 (281-2), anti-CD38 (90), anti-GL7 (GL7), anti-MHC class II (I-A/I-E, M5/114.15.2), anti-CD11c (N418), anti-IgD (11-26c.2a), anti-CD44 (IM7), anti-PD-L2 (TY25), anti-CD80 (16-10A1), anti-CD69 (H1.2F3) and anti-CD86 (GL1) were purchased from BD Biosciences, e-Bioscience or BioLegend. Alexa-Fluor-488-conjugated goat anti-mouse IgG (H+L) was purchased from Invitrogen (ThermoFischer Scientific). Alexa-Fluor-647-conjugated donkey anti-mouse IgG (H+L) antigen-binding fragment (Fab) was purchased from Jackson ImmunoResearch Laboratories. For chemokine receptor staining, anti-CCR1 (643854), anti-CCR2 (475301), anti-CCR3 (83103), anti-CCR4 (2G12), anti-CCR5 (HM-CCR5), anti-CCR6 (29-2L17), anti-CCR7 (4B12), anti-CCR8 (SA214G2), anti-CCR9 (CW-1.2), anti-CCR10 (248918), anti-CXCR1 (1122A), anti-CXCR2 (TG11), anti-CXCR3 (CXCR3-173), anti-CXCR4 (2B11/CXCR4), anti-CXCR5 (L138D7) and anti-CXCR6 (SA051D1) were purchased from BioLegend, BD Biosciences or R&D systems. For intracellular staining, anti-IFNγ (XMG1.2) was purchased from BioLegend.

Isolation of leukocytes from vaginal tissues, cervix and uterus. The genital tracts of vaginal tissues and upper reproductive tracts, including cervix and uterus, treated with Depo-Provera were dissected. Tissues were then incubated with 0.5 mg/ml Dispase II (Roche) for 15 min at 37 °C. Thereafter, tissues were digested with 1 mg/ml collagenase D (Roche) and 30 μg/ml DNase I (Sigma-Aldrich) at 37 °C for 25 min. The resulting cells were filtered through a 70-μm filter and single cells were isolated as previously described[32].

Flow cytometry. Preparation of single-cell suspensions from vagina, cervix and uterus were described above. Blood collected in PBS including 2 mM EDTA was treated with ACK lysis buffer 3 times for single-cell preparation. Single cells were pretreated with anti-CD16/32 antibody (2.4G2) to block Fc receptors, and stained with the antibodies. Live versus dead cells were stained with LIVE/DEAD fixable Aqua dead cell stain kit (Invitrogen). Multiparameter analyses were carried out on the LSR II flow cytometer (Becton Dickinson) and were analysed using the FlowJo software (Tree Star). To stain intracellular IFNγ, single-cell suspensions from vaginal tissues of TK$^-$ HSV-2 immunized mice were stimulated in the presence of 5 μg/ml brefeldin A with naive splenocytes (CD45.1$^+$) loaded with heat-inactivated HSV-2 antigen (0.5 pfu equivalent per cell) for 10–12 h (ref. [14]). Cells were surface-stained with anti-CD3ε (145-2C11), anti-CD4 (GK1.5 and RM4-5) and anti-CD44 (IM7), and then fixed and permeabilized using a Cytofix/Cytoperm Fixation/Permeabilization kit (BD Biosciences) according to the manufacturer's instructions. These cells were intracellular stained with anti-IFNγ (XMG1.2).

Quantitative reverse-transcription polymerase chain reaction. Vaginal tissues were lysed in RLT lysis buffer and RNA was isolated using RNeasy mini kit (Qiagen), according to the manufacturer's instructions. Contaminating DNA was removed using recombinant DNaseI (Roche), and cDNA was generated with iScript cDNA synthesis kit (BioRad), each according to the manufacturer's instructions. Quantitative PCR was performed using SYBR green-based quantification (Qiagen). Expression of mRNA of various chemokines in vaginal tissues was quantitated by quantitative reverse-transcription PCR (RT–qPCR) using the following set of primers: *Cxcl9* (F, cgagaccatttactgcaacag; R, taattgggccaacagtagcc), *Cxcl10* (F, gctgcaactgcatccatatc; R, gtggcaatgatctcaacacg), *Cxcl11* (F, cgggatgaaagccgtcaa; R, tatgaggcgagcttgcttgg), *Ccl20* (F, atggcctgcggtggcaagcgtctg; R, taggctgaggaggttcacagccct) and *Cxcl13* (F, ctctccaggccacggtatt; R, taaccatttggcacgaggat). Expression of target genes was normalized against housekeeping gene *Hprt*.

Bone marrow chimeric mice. Bone marrow chimeric mice, using C57BL/6, CD11b DTR, μMT and *Cxcr3*$^{-/-}$ mice, were constructed by a standard method[29]. In brief, the recipient mice were irradiated with two doses of 4.75 Gy or 6.00 Gy each, 3 h apart. Irradiated recipient mice were reconstituted with 5×10^6–1×10^7 cells of the appropriate cell suspension by means of intravenous injection. The reconstituted mice were maintained in a clean facility for at least eight weeks before use.

Adoptive transfer of B cells. B cells were isolated from spleens of DsRed mice immunized intravaginally with 10^5 pfu of TK$^-$ HSV-2 five weeks prior, using EasySep Mouse B cell Isolation Kit (STEMCELL Technologies) according to the manufacturer's instructions. At the indicated hours post-challenge, 5×10^6 isolated B cells were transferred into C57BL/6 mice immunized intravaginally with 10^5 pfu of TK$^-$ HSV-2 five weeks previously. Mice were killed two hours later and vaginal tissues were analysed for the presence of donor B cells.

In vivo treatment with toxins, antibodies, FTY720 and CpG1826. To deplete CD11b$^+$ cells, CD11bDTR chimeric mice were treated with 10 ng/g body weight intravenously on days −4 and −1, and 50 ng diphtheria toxin (Sigma) intravaginally on days −4, −3, −2 and −1. To deplete CD4 T cells, mice were treated with 300 μg intravenously on day −4 and −1, and 10 μg anti-mouse CD4 antibody (GK1.5, BioXCell) intravaginally for four consecutive days before virus challenge. For neutralization of IFNγ, mice were treated with 500 μg intravenously on day −4 and −1, and 10 μg anti-mouse IFNγ antibody (R4-6A2, BioXCell) intravaginally for four consecutive days before virus challenge. For fluorescent antibody injection, mice were injected intravenously with 200 μg of FITC-conjugated mouse IgG antibody (Jackson ImmunoResearch). For HSV-2 monoclonal antibody treatment, mice were injected intravenously or intravaginally with 1 μg of mouse IgG1 monoclonal antibody specific for glycoprotein D (gD) of HSV (E317, Absolute Antibody). Thirty seconds after intravaginal injection or 3 h after intravenous injection of monoclonal antibody, mice were infected intravaginally with 2,500 pfu of wild-type HSV-2. For FTY720 treatment, immunized mice were given drinking water containing 4 μg/ml of FTY720 (Cayman Chemical) for 2 weeks. For CpG1826 treatment, mice were injected intravaginally with 100 μg of CpG1826 (TriLink BioTechnologies).

ELISA. Vaginal fluids were collected from the indicated days after infection by using calcium alginate swabs and pipetting PBS into and out of the vagina 20 times. Bronchoalveolar lavage fluids were collected by washing the trachea with 1 ml of PBS containing 0.1% BSA. A ninety-six-well EIA/RIA plate was coated with 100 μl of heat-inactivated or PFA-inactivated purified HSV-2 (10^4 to 10^5 pfu equivalent per 100 μl) or PFA-inactivated influenza A/PR8 virion (10^5 pfu equivalent per 100 μl) for virus-specific immunoglobulin measurement or goat anti-mouse immunoglobulin (1:1,000; SouthernBiotech, 1010-01) for total immunoglobulin measurement in carbonate buffer (pH 9.5) and then incubated overnight at 4 °C. On the following day, these plates were washed with PBS-Tween 20 and blocked for 2 h with 5% FBS in PBS. Wash and serum samples were then plated in the wells and incubated for at least four hours at ambient temperature. After washing in PBS-Tween 20, HRP-conjugated anti-mouse IgG1, IgG3, IgM, IgA, IgG2b or IgG2c (SouthernBiotech) was added in the wells for 1 h, followed by washing and adding TMB solution (eBioscience). Reactions were stopped with 1 N H_2SO_4 and absorbance was measured at 450 nm. The total antibody titres were defined by using immunoglobulin standard (C57BL/6 Mouse Immunoglobulin Panel; SouthernBiotech). The levels of CXCL9 and CXCL10 in vaginal fluids were measured using DuoSet ELISA kit (R&D Systems) according to manufacturer's instructions.

Immunofluorescence staining. For tissue staining, frozen sections of vagina, spleen and lung collected from various experimental groups were stained with the antibody (anti-CD4 (H129.19)) in a previously described procedure[29]. Likewise, FITC, CD138, B220, CD31, VCAM-1, IgG2b, IgG2c, total IgG and HSV-2

antigens were detected using Alexa-Fluor-647-conjugated anti-FITC antibody, biotin-conjugated anti-mouse CD138 antibody (281-2), PE-conjugated anti-mouse B220 antibody (RA3-6B2), biotin-conjugated anti-mouse CD31 antibody (390), biotin-conjugated anti-VCAM-1 antibody (429/MVCAM.A), HRP-conjugated IgG2b and IgG2c (SouthernBiotech), Alexa-Fluor-568-conjugated anti-mouse IgG (H+L) (Invitrogen) and FITC-conjugated polyclonal antibodies against HSV-1 and HSV-2 (ViroStat). Stained slides were washed and incubated with DAPI, and mounted with Fluoromount-G (SouthernBiotech). Images were captured using a 10× or 40× objective lens from fluorescence microscopy (BX51; Olympus).

Induction of breach of the epithelial layer, and haematoxylin and eosin stain. The vaginal tracts of mice immunized subcutaneously with 10^6 pfu of TK^- HSV-2 five weeks previously were brushed with an interdental brush. The vaginal tracts were washed with PBS after brushing for immunoglobulin ELISA, and vaginal tissues were embedded in paraffin blocks and sectioned by the Yale Pathology Tissue Services. Haematoxylin and eosin (H&E) staining was performed by the Yale Pathology Tissue Services. H&E images were captured using light microscopy (BX51; Olympus).

scRNA-seq sample preparation. Naive mice or mice immunized with 10^5 pfu of TK^- HSV-2 5 weeks previously were infected with 10^5 pfu of wild-type HSV-2. One day later, single cells from vaginal tissue and spleen were isolated and surface-stained with anti-CD45 (30-F11), anti-CD3ε (145-2C11), anti-CD4 (GK1.5), anti-CD8α (53-6.7) and anti-CD19 (1D3) for vagina, and anti-CD45 (30-F11), anti-CD19 (6D5 and 1D3), anti-CD38 (90), anti-GL7 (GL7), anti-MHC class II (I-A/I-E, M5/114.15.2) and anti-IgD (11-26c.2a) for spleen. Stained cells were sorted by FACS Aria (BD Biosciences). $CD45^+CD3\varepsilon^+CD4^+$, $CD45^+CD3\varepsilon^+CD8\alpha^+$ and $CD45^+CD3\varepsilon^-CD19^+$ cells (vagina) and $CD45^+CD19^+IgD^-IgG^+MHCII^+GL7^-CD38^+$ cells (spleen) were collected for further analysis. For B-cell-sorted spleen samples, cell numbers were counted and 6,000 cells were prepared. Cells from primary- and secondary-infected FRT samples were prepared at a cell count proportional to the immune-cell infiltration observed by flow cytometry. Single-cell suspensions were loaded onto the Chromium Controller (10x Genomics) for droplet formation. scRNA-seq libraries were prepared using the Chromium Single Cell 5′ Reagent Kit (10x Genomics) and Single Cell V(D)J Kit, according to manufacturer's protocol. Samples were sequenced on the HiSeq4000 with 28-bp read 1, 8-bp i7 index and 98-bp read 2 for the gene-expression library, and on the NovaSeq with 150 paired reads for BCR library.

scRNA-seq analysis. R v.3.4.2 (R Core Team 2013) and Python 3.5.4 (2017) was used for all statistical analysis. Sequencing results were demultiplexed into Fastq files using the Cell Ranger (10x Genomics, 2.2.0) mkfastq function. Samples were aligned to mm10-2.2.0 10x genome. The count matrix was generated using the count function with default settings. Matrices were loaded into Seurat v.2[33] for downstream analysis. Cells with less than 500 unique molecular identifiers, or high mitochondrial content were discarded. For principal component analysis, variable genes were analysed using the Jackstraw method. An estimate of 13,763 cells was sequenced (2 conditions and 2 organs), with 45,838 mean reads per cell. Principal component values that were statistically significant were identified, and a cut-off point was determined using the inflection point after using the PCElbowPlot function. Clusters were determined using the FindClusters function in Seurat v.2, which implements a shared nearest neighbour clustering algorithm. For analysis, the Wilcoxon rank-sum test was used for all differentially expressed genes. After this initial analysis, clusters expressing *Cd19* or *Cd3* were separated, and *Cd19*-expressing clusters were re-clustered using the approach described above. Several iterations of the clustering was performed with different resolution, and the cluster of each version was validated by gene expression and relative population size compared to fluorescence-activated cell sorting data, to determine the resolution. Cell types were determined using previously published data sets, gene set enrichment analysis B-cell subtypes (GSE11386, Broad Institute) and ImmGen (Immunological Genome project, Harvard Medical School) as references. An additional clustering was also performed on FRT B cells using the method described above.

B-cell-repertoire analysis. V(D)J germline segments were assigned with IgBLAST v.1.7.0[34] using the 30 March 2017 version of the IMGT gene database. Following V(D)J annotation, cells were assigned into clonal groups using Change-O v.0.4.2[26], which is available as part of the www.Immcantation.org framework. Cells with multiple *Igh* V(D)J sequences were first removed. *Igh* V(D)J sequences were partitioned by common *Igh* V and *Igh* J gene annotations, and nucleotide junction-region length. In addition, *Igh* V(D)J sequences were further grouped based on whether the associated cells shared common combinations of *Igk* V with *Igk* J or *Igl* V with *Igl* J gene annotations. Within these groups, *Igh* sequences with junctions that differed from one another by a length-normalized Hamming distance of less than 0.1 were defined as clones by single-linkage clustering. This threshold was identified by the local minima between the two modes of the within-sample bimodal distance-to-nearest histogram. Germline sequences were reconstructed for each clonal cluster (*Igh* V) with masked D segment and N and P regions (N regions replaced); ambiguous gene assignments within clonal clusters were assigned to majority gene. To calculate confidence intervals for clonal overlap and account for the effect of different sampling depth from each repertoire, clonal overlap of *Igh* V(D)J sequences was bootstrapped (2,000 replicates) using stratified bootstrapping implemented in the boot v.1.3-20 R package with weights to sample the secondary challenge compartments at the same depth as the primary infection compartments. Significance from bootstrap analysis was computed from the empirical cumulative distribution function using a one-tailed test for clonal overlap analysis with a null hypothesis of no overlap. Lineage trees were constructed for clones with more than one sequence using PHYLIP and Alakazam v.0.2.11 in R.

Statistical analysis. Survival curves were analysed using the log-rank test. Disease score and virus titre were analysed using two-way analysis of variance (ANOVA). Others were analysed using two-tailed Mann–Whitney *U* test. Significance from bootstrap analysis was computed from the empirical cumulative distribution function, using a one-tailed test for clonal overlap analysis with a null hypothesis of zero overlap, and a two-tailed test for clonal diversity analysis.

Reporting summary. Further information on research design is available in the Nature Research Reporting Summary linked to this paper.

Data availability

RNA sequencing data are available at BioProject, under accession number PRJNA524497. All datasets generated and/or analysed during the current study are available in the Letter, the accompanying Source Data or Supplementary Information, or are available from the corresponding author upon reasonable request.

Code availability

All R and Python codes used in this analysis are available from the corresponding author upon request.

29. Iijima, N. et al. Dendritic cells and B cells maximize mucosal Th1 memory response to herpes simplex virus. *J. Exp. Med.* **205**, 3041–3052 (2008).
30. Ichinohe, T. et al. Microbiota regulates immune defense against respiratory tract influenza A virus infection. *Proc. Natl Acad. Sci. USA* **108**, 5354–5359 (2011).
31. Iijima, N., Mattei, L. M. & Iwasaki, A. Recruited inflammatory monocytes stimulate antiviral Th1 immunity in infected tissue. *Proc. Natl Acad. Sci. USA* **108**, 284–289 (2011).
32. Iijima, N., Linehan, M. M., Saeland, S. & Iwasaki, A. Vaginal epithelial dendritic cells renew from bone marrow precursors. *Proc. Natl Acad. Sci. USA* **104**, 19061–19066 (2007).
33. Butler, A., Hoffman, P., Smibert, P., Papalexi, E. & Satija, R. Integrating single-cell transcriptomic data across different conditions, technologies, and species. *Nat. Biotechnol.* **36**, 411–420 (2018).
34. Ye, J., Ma, N., Madden, T. L. & Ostell, J. M. IgBLAST: an immunoglobulin variable domain sequence analysis tool. *Nucleic Acids Res.* **41**, W34–W40 (2013).

Acknowledgements We thank M. Linehan and H. Dong for technical assistance, Yale Flow Cytometry Facility, especially G. Lyon, for cell sorting, Yale Center for Genome Analysis (YCGA), especially G. Wang and C. Castaldi, for 10x Chromium library preparations and help with sequencing, P. Wong and T. Mao for helpful discussions regarding the single-cell RNA-seq data, Y. Kong for helpful advice in statistical analysis, and K. B. Hoehn for advice on BCR lineage tree drawing. This study was supported by awards from NIH AI054359, AI062428, AI064705, AI102625 (to A.I.), NIH AI104739 (to S.H.K.), Basic Science Research Program through the National Research Foundation of Korea (NRF-2016R1A6A3A03010349) funded by the Ministry of Education (to J.E.O.), the Japan Agency for Medical Research and Development (AMED) JP18fm0208011h0002, the Japan Society for the Promotion of Science (JSPS) JP18H02857, Takeda Science Foundation (to N.I.), and NIH T32GM007205 (MSTP training Grant) (to E.S. and R.J.). A.I. is an investigator of the Howard Hughes Medical Institute.

Author contributions J.E.O., N.I., E.S. and A.I. designed the experiments; J.E.O., N.I., E.S., R.J. and A.I. prepared the manuscript; J.E.O., N.I., P.L. and J.K. performed experiments; J.E.O., N.I. and A.I. analysed data; and E.S., R.J. and S.H.K. analysed single-cell RNA-seq data.

Competing interests The authors declare no competing interests.

Additional information

Supplementary information. is available for this paper at https://doi.org/10.1038/s41586-019-1285-1.

Correspondence and requests for materials should be addressed to A.I.

Peer review information *Nature* thanks Harvey Friedman and the other anonymous reviewer(s) for their contribution to the peer review of this work.

Reprints and permissions information is available at http://www.nature.com/reprints.

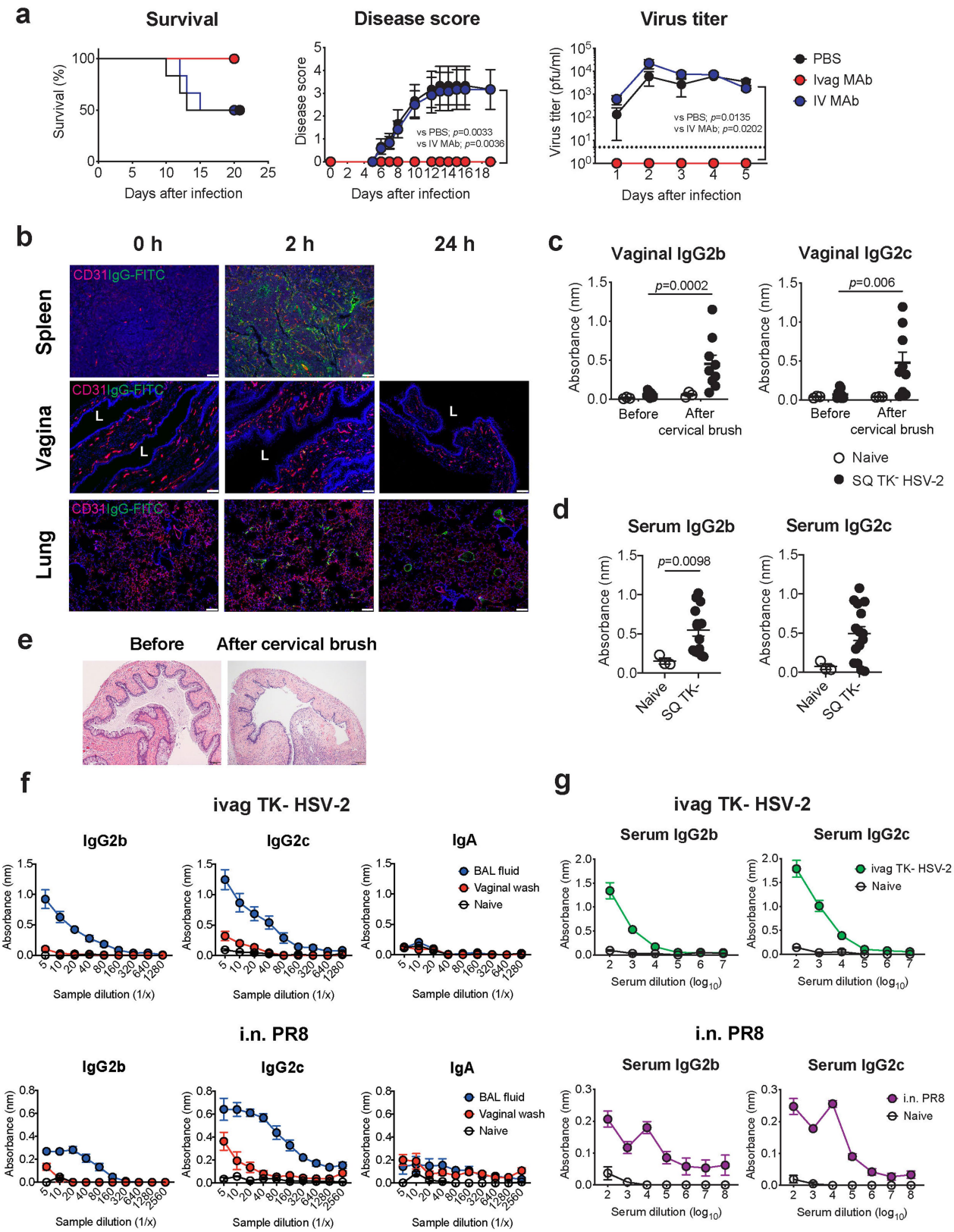

Extended Data Fig. 1 | See next page for caption.

Extended Data Fig. 1 | Circulating antibodies are incapable of entering the vaginal mucosal lumen in the absence of minor abrasion. **a**, C57BL/6 mice treated intravaginally or intravenously with HSV-gD-specific monoclonal antibody were infected with intravaginal wild-type HSV-2. Survival, disease severity and virus titre in vaginal wash were analysed ($n = 6$ mice). The dashed line indicates the limit of detection. **b**, C57BL/6 mice treated with Depo-Provera were injected intravenously with FITC-conjugated mouse IgG antibody. Frozen sections of vagina, spleen and lung were stained with anti-CD31 (red), anti-FITC (green) antibodies, and DAPI (blue). L indicates vaginal lumen. Scale bars, 100 μm. **c**–**e**, C57BL/6 mice were immunized subcutaneously with TK^- HSV-2. Five weeks later, the vaginal tract of immunized mice with Depo-Provera treatment was brushed with a cervical brush to make a breach, or to create minor abrasions of the epithelial barrier of the vaginal mucosa. HSV-specific antibodies in vaginal wash before and after cervical brush (**c**; naive; $n = 3$ mice; subcutaneous (SQ) TK^- HSV-2, $n = 9$ mice) and in serum (**d**; naive; $n = 3$ mice; subcutaneous TK^- HSV-2, $n = 15$ mice) were measured by ELISA. Sample dilution for ELISA was 1:2 (vaginal wash) or $1:10^3$ (serum). **e**, H&E stain of the vagina before and after breach was performed in mice with Depo-Provera treatment. **f**, **g**, C57BL/6 mice were immunized intravaginally with TK^- HSV-2 or intranasally (i.n.) with influenza A strain PR8 (H1N1) virus. Five weeks later, virus-specific antibodies in bronchoalveolar lavage (BAL) fluid, vaginal wash (**f**; naive, $n = 4$ mice; intravaginal TK^- HSV-2, $n = 6$ mice; intranasal PR8, $n = 4$ mice) and blood (**g**; naive mice, $n = 4$ mice; intravaginal TK^- HSV-2, $n = 13$ mice; intranasal PR8, $n = 8$ mice) were measured by ELISA. Data are mean ± s.e.m. Data are representative of two independent experiments (**a**, **b**, **e**) or are pooled from two independent experiments (**c**, **d**, **f**, **g**). Statistical significance was analysed by two-way analysis of variance (ANOVA) (**a**; disease score and virus titre), log-rank (Mantel–Cox) test (**a**; survival) or two-tailed Mann–Whitney *U* test (**c**, **d**).

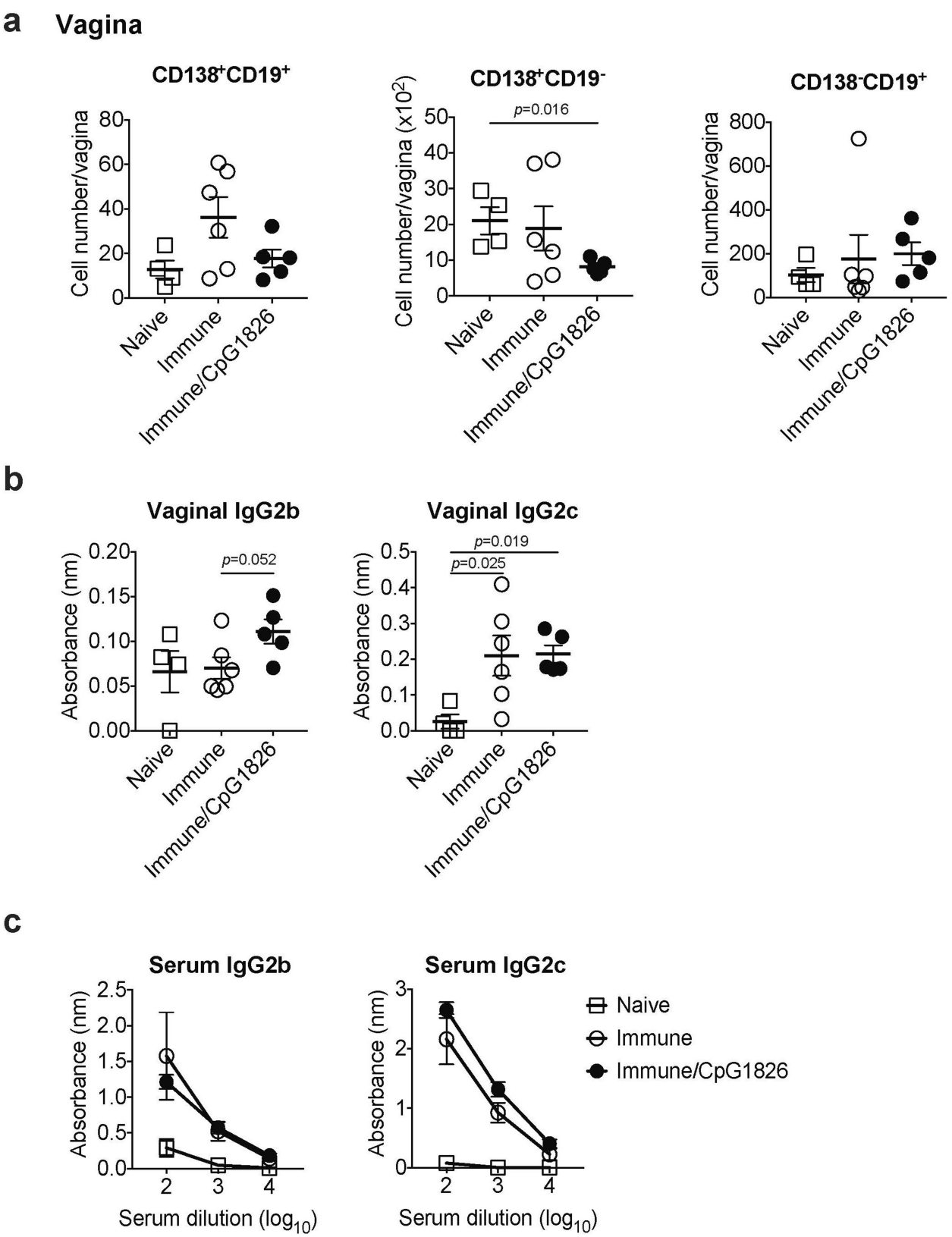

Extended Data Fig. 2 | The vagina is devoid of virus-specific antibodies and tissue-resident B cells even after boosting local inflammation after immunization with HSV-2. C57BL/6 mice were immunized intravaginally with TK$^-$ HSV-2. On day 5 after immunization, CpG1826 was injected into the vagina to boost local inflammation of the vaginal mucosa. **a**, Five weeks later, the number of CD138$^+$CD19$^+$, CD138$^+$CD19$^-$ and CD138$^-$CD19$^+$ cells in vaginal tissues was analysed by flow cytometry (naive, $n = 4$ mice; immune, $n = 6$ mice; immune and CpG1826, $n = 5$ mice). **b**, **c**, HSV-2-specific antibodies in vaginal wash (**b**; naive, $n = 4$ mice; immune, $n = 6$ mice; immune and CpG1826, $n = 5$ mice) and in serum (**c**; naive, $n = 3$ mice; immune, $n = 3$ mice; immune and CpG1826, $n = 5$ mice) were measured by ELISA. Sample dilution for the vaginal wash ELISA was 1:5. Data are mean ± s.e.m. Data are representative of two independent experiments. Statistical significance was analysed by two-tailed Mann–Whitney *U* test.

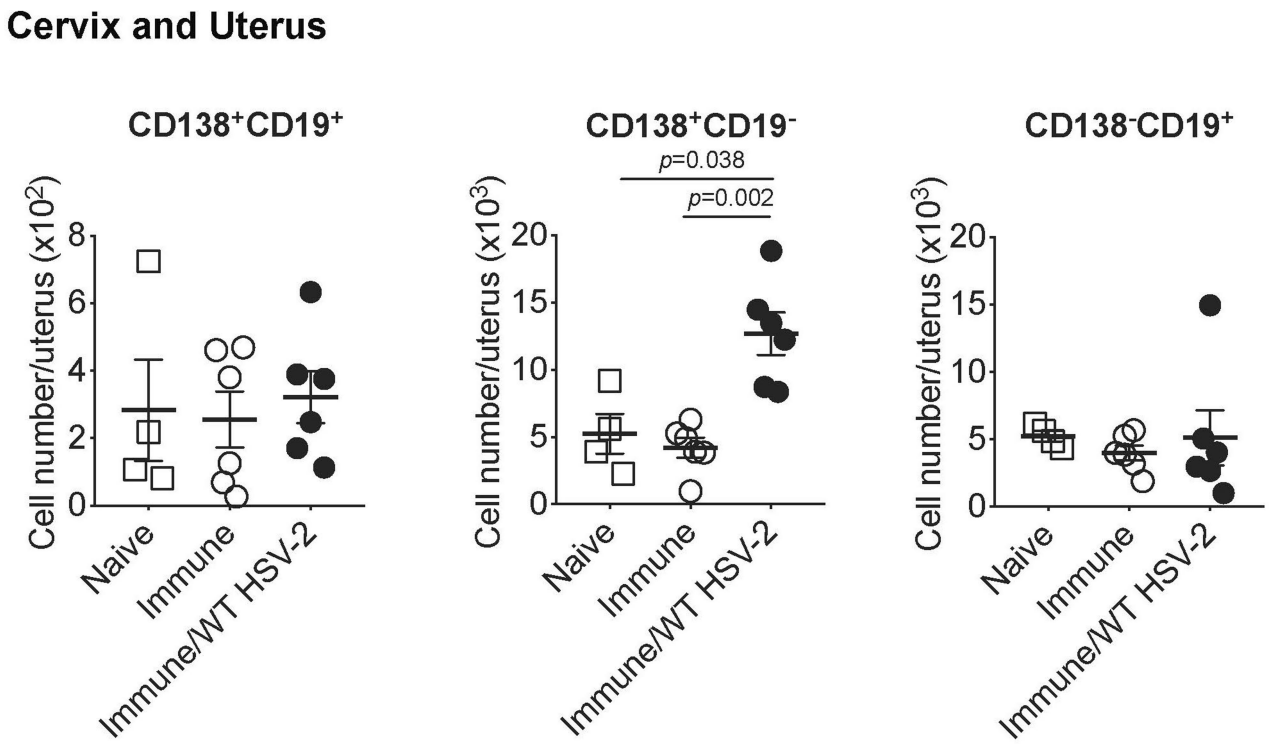

Extended Data Fig. 3 | B cells do not establish residency in the upper reproductive tract following immunization and challenge with HSV-2. C57BL/6 mice were immunized intravaginally with TK$^-$ HSV-2. Five weeks later, mice were challenged with intravaginal wild-type HSV-2. One day after challenge, the number of CD138$^+$CD19$^+$, CD138$^+$CD19$^-$ and CD138$^-$CD19$^+$ cells in cervix and uterus was analysed by flow cytometry (naive, $n = 4$ mice; immune, $n = 6$ mice; immune and wild-type HSV-2, $n = 6$ mice). Data are mean ± s.e.m. Data are pooled from two independent experiments. Statistical significance was analysed by two-tailed Mann–Whitney *U* test.

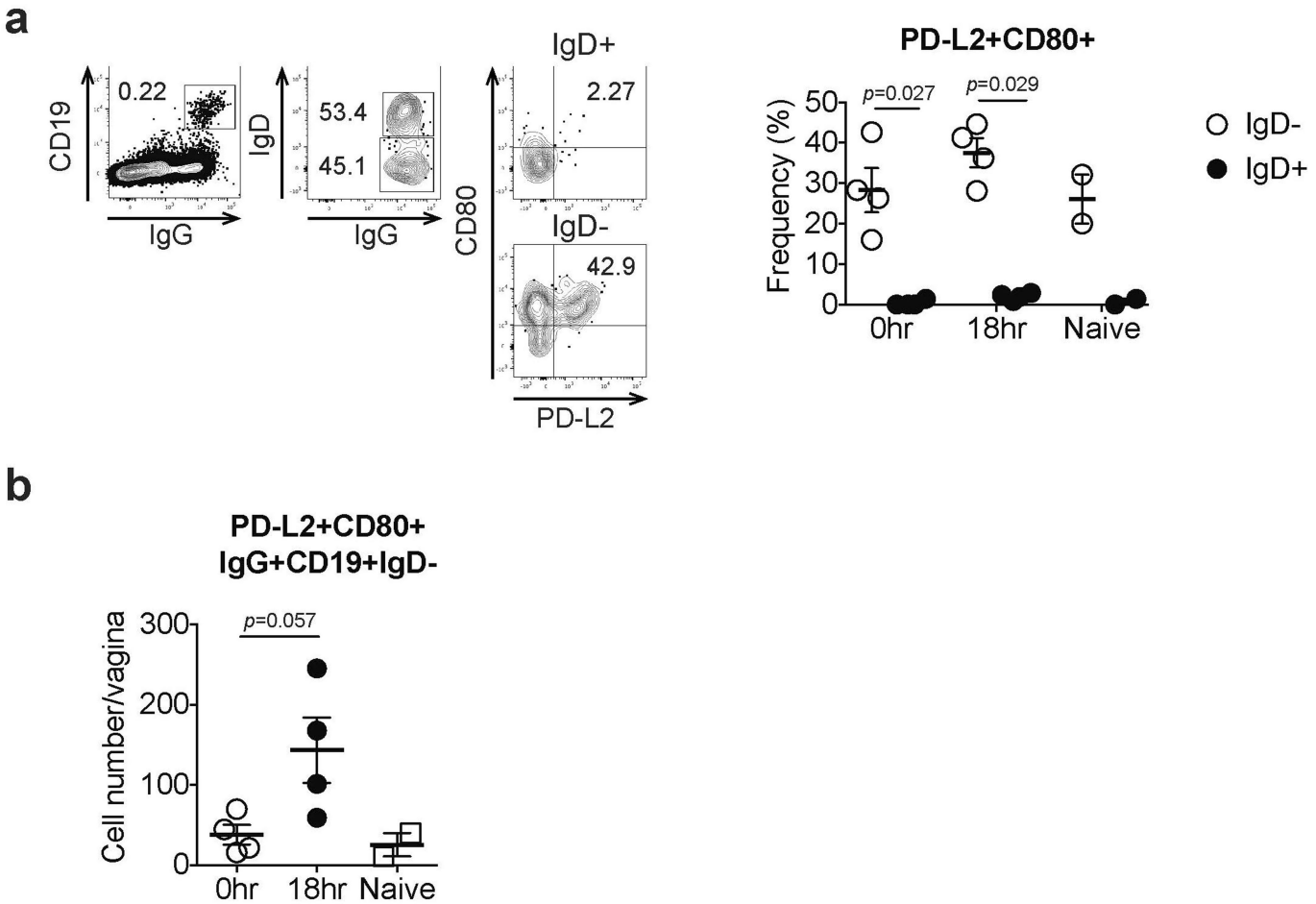

Extended Data Fig. 4 | Surface-marker profiles of recruited memory B cells in the vagina. C57BL/6 mice immunized with TK$^-$ HSV-2 five weeks previously were challenged with wild-type HSV-2. **a**, Eighteen hours later, CD80 and PD-L2 expression on both IgD$^+$ and IgD$^-$ B cells in vaginal tissues was analysed by flow cytometry. **b**, The number of CD80$^+$PD-L2$^+$ memory B cells in the vagina at 18 h after secondary challenge was analysed by flow cytometry (naive, $n = 2$ mice; immune, $n = 4$ mice). Data are mean ± s.e.m. Data are representative of two independent experiments. Statistical significance was analysed by two-tailed Mann–Whitney *U* test.

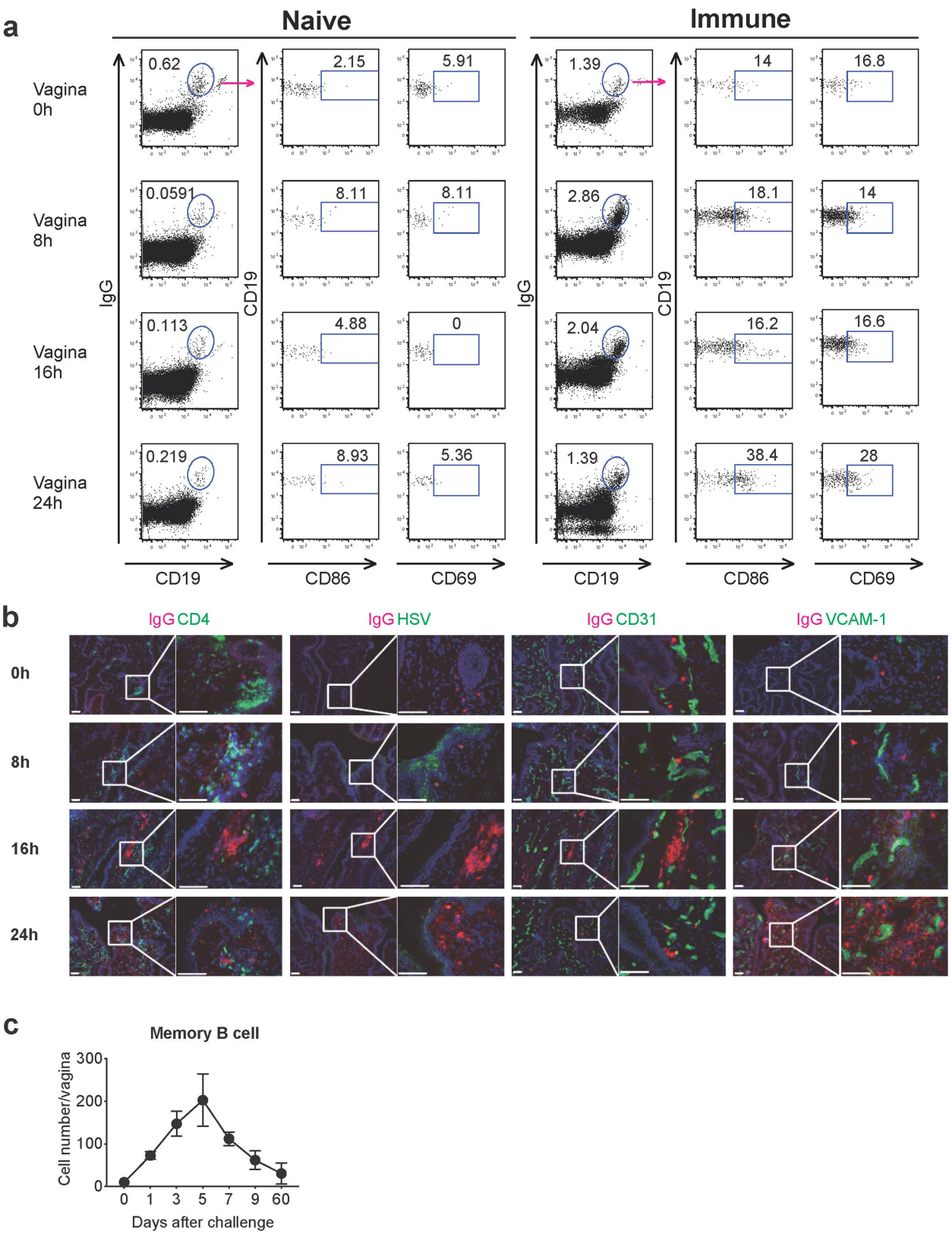

Extended Data Fig. 5 | Migrated B cells rapidly activate in the vagina and remain for several weeks. a, Naive C57BL/6 mice or C57BL/6 mice immunized with TK$^-$ HSV-2 five weeks previously were challenged with wild-type HSV-2. Eight, sixteen and twenty-four hours after challenge, CD86 and CD69 expression on IgD$^-$IgG$^+$ memory B cells in vaginal tissues was analysed by flow cytometry. **b**, C57BL/6 mice were immunized vaginally with TK$^-$ HSV-2 five weeks prior. After challenge, frozen sections of vagina were stained with antibodies against IgG (red), CD4, HSV, CD31 and VCAM-1 (green), and DAPI (blue). Scale bars, 100 μm. **c**, C57BL/6 mice immunized with TK$^-$ HSV-2 five weeks previously were challenged with wild-type HSV-2. At the indicated days after challenge, the number of memory B cells in vaginal tissues was analysed by flow cytometry ($n = 2$–4 mice in each time point). Data are mean ± s.e.m. Data are representative of two independent experiments.

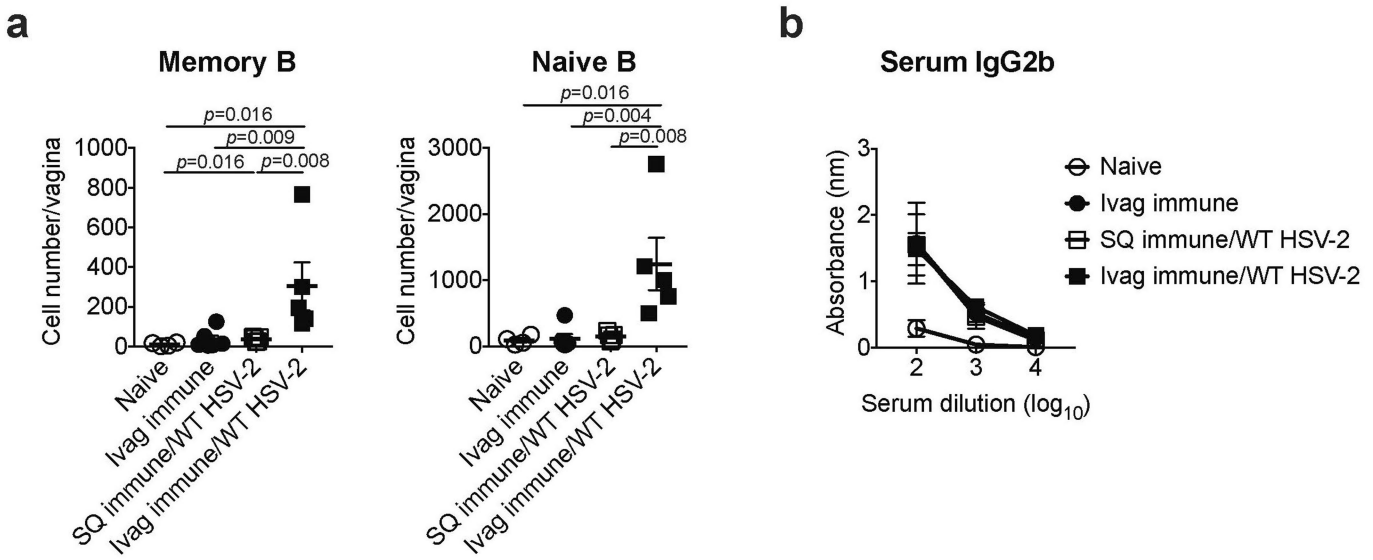

Extended Data Fig. 6 | Local intravaginal immunization with HSV-2 is required for the recruitment of memory B cells. C57BL/6 mice were immunized intravaginally or subcutaneously with TK$^-$ HSV-2. Five weeks later, mice were challenged with wild-type HSV-2. **a**, One day after challenge, the number of memory and naive B cells in vaginal tissues was analysed by flow cytometry (naive, $n = 4$ mice; intravaginal immune, $n = 6$ mice; subcutaneous immune and wild-type HSV-2, $n = 5$ mice; intravaginal immune and wild-type HSV-2, $n = 5$ mice). **b**, HSV-2-specific IgG2b antibody in serum was measured by ELISA (naive, $n = 3$ mice; intravaginal immune, $n = 3$ mice; subcutaneous immune and wild-type HSV-2, $n = 5$ mice; intravaginal immune and wild-type HSV-2, $n = 3$ mice). Data are mean ± s.e.m. Data are representative of two independent experiments. Statistical significance was analysed by two-tailed Mann–Whitney *U* test.

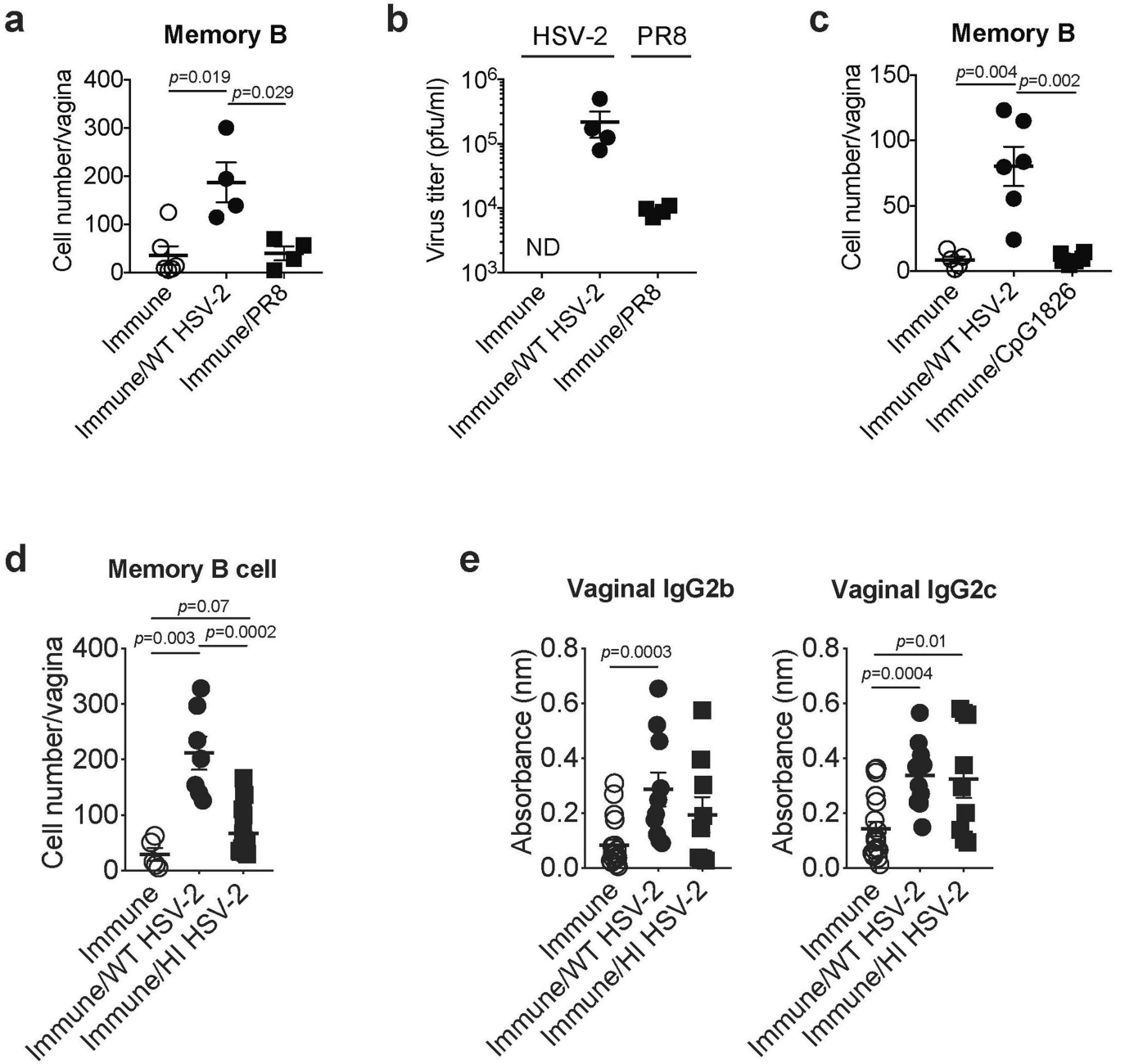

Extended Data Fig. 7 | Antigen-specific recall response is necessary for the recruitment of memory B cells. a, **b**, C57BL/6 mice immunized with intravaginal TK$^-$ HSV-2 five weeks previously were challenged with wild-type HSV-2 or influenza A strain PR8 virus intravaginally (immune, $n = 6$ mice; immune and wild-type HSV-2, $n = 4$ mice; immune and PR8, $n = 4$ mice). **a**, One day after secondary challenge, the number of memory B cells in vaginal tissues was analysed by flow cytometry. **b**, Indicated virus titre in vaginal wash was measured one day after secondary challenge. **c**, C57BL/6 mice immunized intravaginally with TK$^-$ HSV-2 five weeks previously were challenged with wild-type HSV-2 or CpG1826 intravaginally. One day after secondary challenge, the number of memory B cells in vaginal tissues was analysed by flow cytometry (immune, $n = 5$ mice; immune and wild-type HSV-2, $n = 6$ mice; immune and CpG1826, $n = 6$ mice). **d**, **e**, C57BL/6 mice immunized intravaginally with TK$^-$ HSV-2 five weeks previously were intravaginally challenged with active or heat-inactivated (HI) wild-type HSV-2. **d**, One day after secondary challenge, the number of memory B cells in vaginal tissues was analysed by flow cytometry (immune, $n = 5$ mice; immune and wild-type HSV-2, $n = 7$ mice; immune and heat-inactivated HSV-2, $n = 14$ mice). **e**, One day after challenge, HSV-2-specific antibodies in vaginal wash were measured by ELISA (immune, $n = 19$ mice; immune and wild-type HSV-2, $n = 10$ mice; immune and heat-inactivated HSV-2, $n = 9$ mice). Sample dilution for ELISA was 1:5. Data are mean ± s.e.m. Data are representative of two independent experiments (**a**–**c**) or are pooled from three independent experiments (**d**, **e**). Statistical significance was analysed by two-tailed Mann–Whitney *U* test.

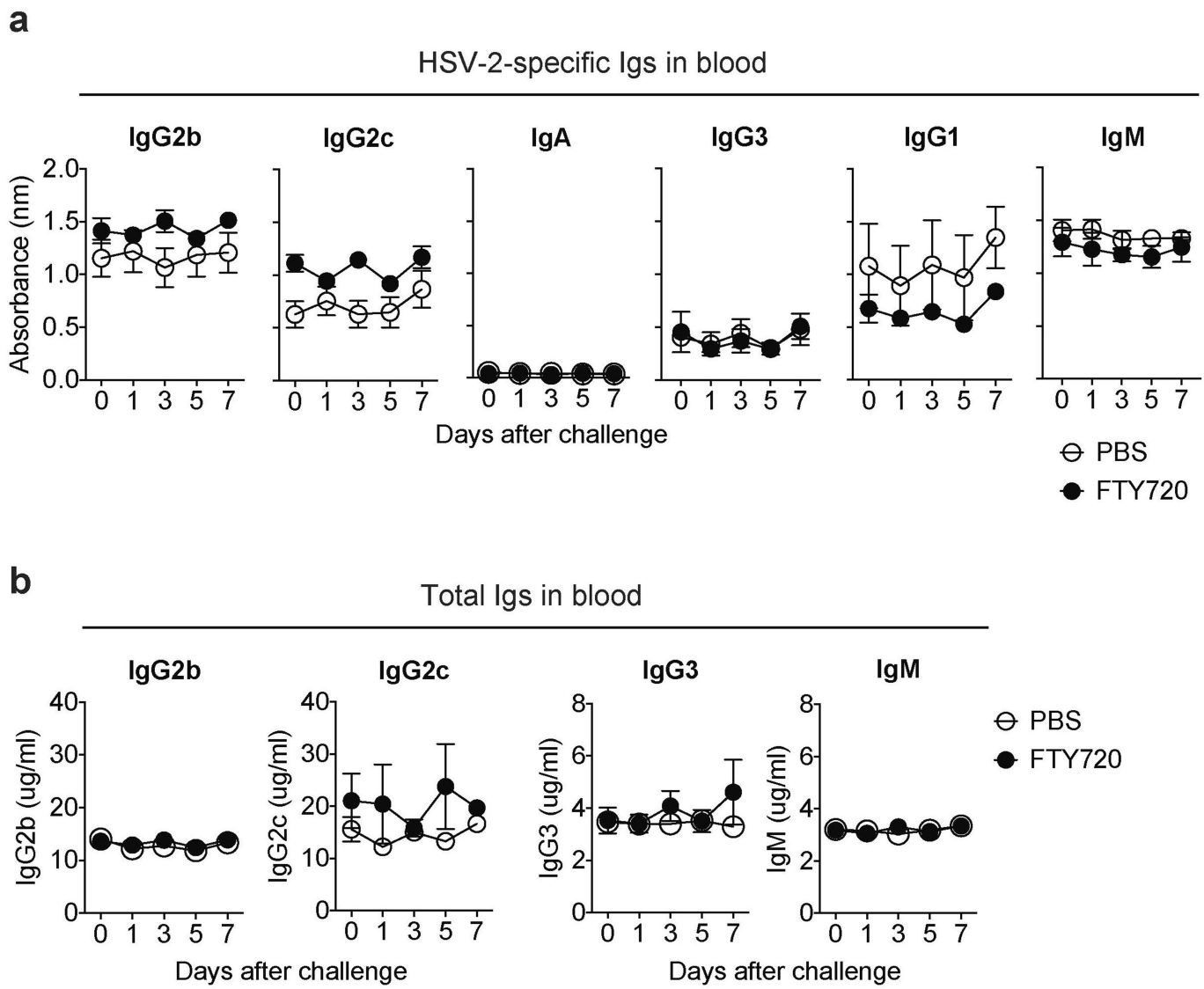

Extended Data Fig. 8 | FTY720 treatment has no effect on circulating antibody levels. C57BL/6 mice were infected vaginally with TK^- HSV-2. Six weeks later, immunized mice were given drinking water containing 4 μg ml^{-1} of FTY720. Two weeks later, FTY720-treated mice were challenged intravaginally with wild-type HSV-2 (10^4 pfu). At the indicated days after challenge, HSV-2-specific antibodies (**a**) and total antibodies (**b**) in the blood were measured by ELISA. Sample dilution for virus-specific antibody ELISA was 1:140. Data are mean ± s.e.m. Data are representative of two independent experiments with 3 mice per group.

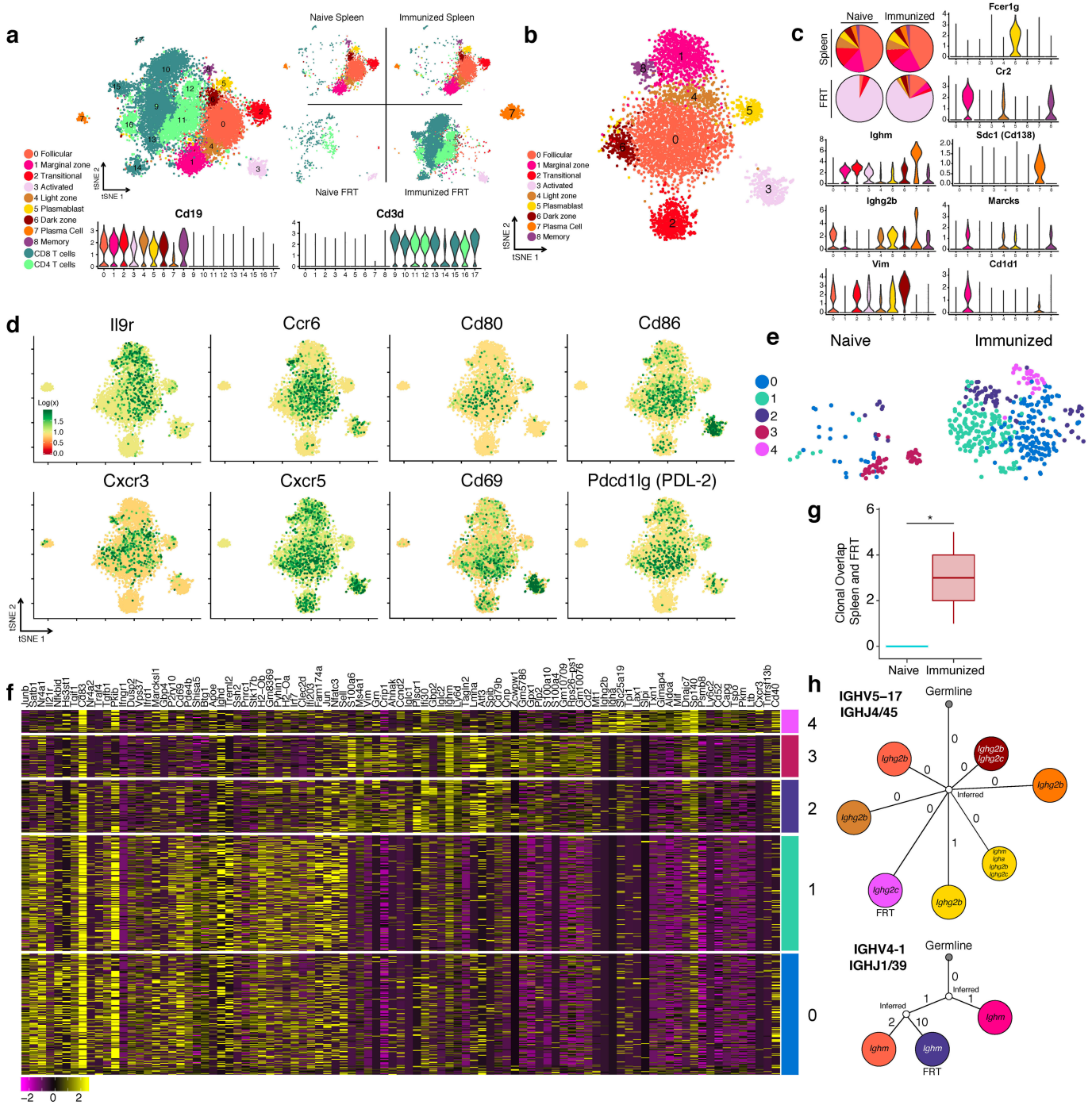

Extended Data Fig. 9 | scRNA-seq analysis reveals unique features associated with memory B cells recruited to the FRT. Spleens and FRT of C57BL/6 mice were collected for 10x Genomics scRNA-seq one day after (re-)challenge with HSV-2; spleens were sorted for B cells and FRTs were sorted for B and T cells ($n = 8$ pooled mice). **a**, *t*-distributed stochastic neighbour-embedding (*t*-SNE) plot associated with 5′ gene-expression profiling of 13,763 cells captured on the 10x Chromium platform. B-cell identities were determined by re-clustering CD19$^+$ populations after initial clustering, and reassigning them according to the analysis in **b** (see Methods). Violin plots depict kernel density estimates to show the distribution of expression values, and were generated using the default VlnPlot function in Seurat ($n = 13,763$ cells). **b**, *t*-SNE plot associated with CD19$^+$ clusters identified from **a** after re-clustering ($n = 5,390$ cells). **c**, Relative cell-population frequency in the different compartments and conditions are shown in pie charts, and the gene expression of each cluster is shown in violin plots. Violin plots depict kernel density estimates to show the distribution of expression values, and were generated using the default VlnPlot function in Seurat ($n = 5,390$ cells). **d**, Heat maps of genes in B cells associated with activation and chemokine or cytokine receptors ($n = 5,390$ cells). **e**, *t*-SNE plots of B cells found in the FRT of naive infected and immunized re-challenged mice after re-clustering only B cells from the FRT ($n = 517$ cells). **f**, Heat map of the top differentially expressed genes in each cluster in **e**. **g**, Clonal overlap between the spleen and the FRT of mice after primary or secondary challenge was measured using single-cell BCR sequencing data, confidence intervals for clonal overlap were computed by bootstrap analysis and significance was assessed for the null hypothesis of zero overlap after secondary challenge ($P = 0.003$). Clonal overlap was computed from all productive BCR sequences from the 5,390 cells. Box plots depict the number of clonal overlaps calculated from bootstrap analysis with whiskers depicting upper percentile of 95th and lower percentile of 5th, and box depicting 80th and 20th percentiles. **h**. Lineage tree of clones that were shared in the spleen and FRT compartment; colours of cell types for splenic B cells and FRT B cells correspond to legends in **c** and **e**, respectively.

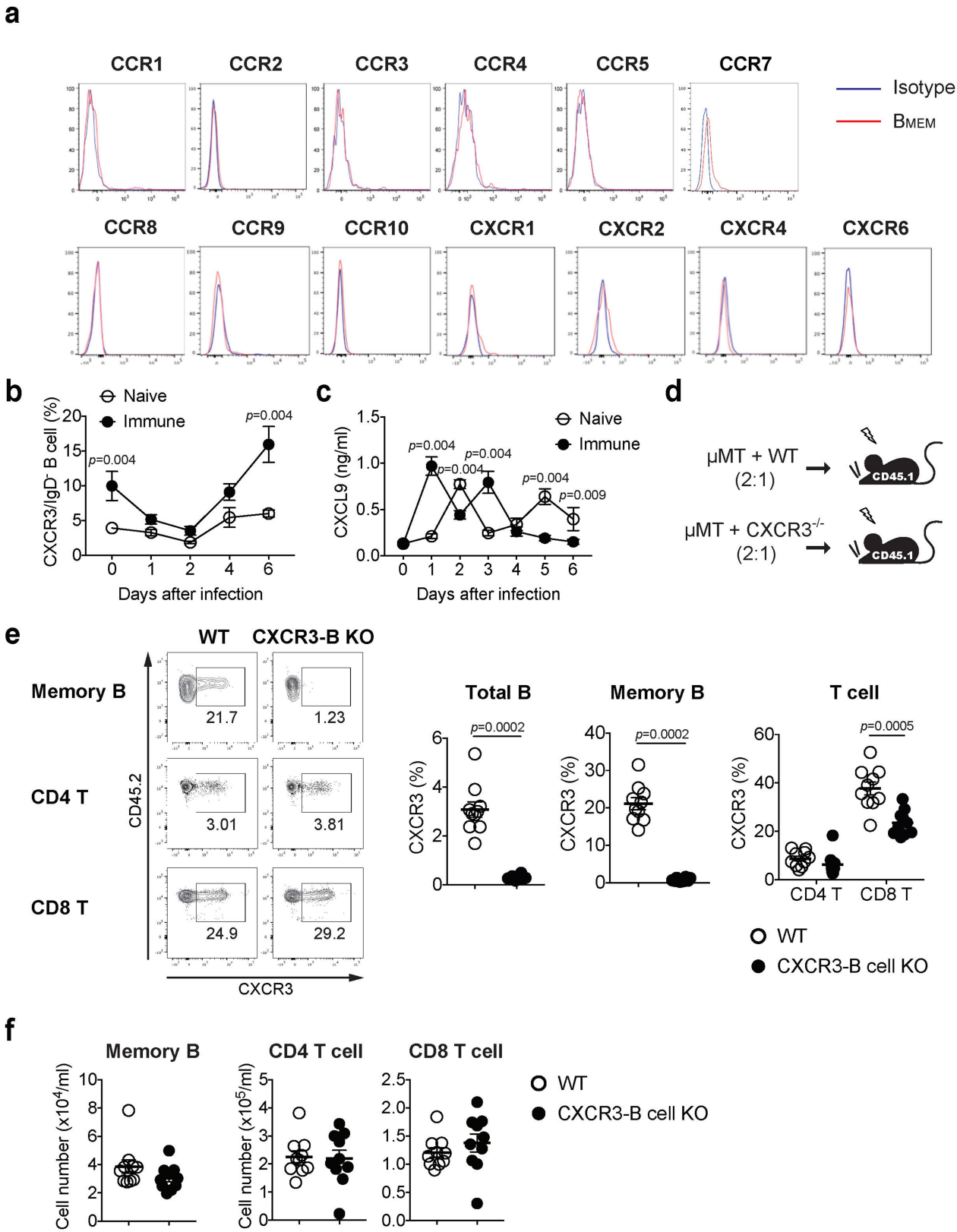

Extended Data Fig. 10 | See next page for caption.

Extended Data Fig. 10 | Surface chemokine receptors on circulating memory B cells, and validation of CXCR3 deficiency and its effect on the number of circulating memory B cells. **a**, C57BL/6 mice were immunized intravaginally with TK^- HSV-2. Five weeks later, the expression of various chemokine receptors on circulating IgD^-IgG^+ memory B cells in blood was analysed by flow cytometry. **b**, **c**, C57BL/6 mice with ($n = 6$) or without ($n = 5$) immunization with TK^- HSV-2 five weeks previously were challenged intravaginally with wild-type HSV-2. At the indicated days following challenge, CXCR3 expression on IgD^-IgG^+ memory B cells was analysed by flow cytometry (**b**) and CXCL9 secretion in vaginal wash was measured by ELISA (**c**). **d**, Strategy for generating mixed bone-marrow chimeric mice. **e**, **f**, Wild-type mice and chimeric mice that lacked CXCR3 only on B cells (CXCR3-B cell KO) were immunized intravaginally with TK^- HSV-2 ($n = 10$ mice). **e**, Five weeks later, CXCR3 expression on IgD^-IgG^+ memory B cells, CD4 T cells and CD8 T cells were analysed by flow cytometry. **f**, Five weeks later, the number of circulating memory B cells, CD4 T cells and CD8 T cells was analysed by flow cytometry. Data are mean ± s.e.m. Data are representative of four (**a**) and two (**b**, **c**) independent experiments or are pooled from two independent experiments (**e**, **f**). Statistical significance was analysed by two-tailed Mann–Whitney *U* test.

nature research

Corresponding author(s): Akiko Iwasaki

Last updated by author(s): Apr 25, 2019

Reporting Summary

Nature Research wishes to improve the reproducibility of the work that we publish. This form provides structure for consistency and transparency in reporting. For further information on Nature Research policies, see Authors & Referees and the Editorial Policy Checklist.

Statistics

For all statistical analyses, confirm that the following items are present in the figure legend, table legend, main text, or Methods section.

n/a	Confirmed	
☐	☒	The exact sample size (*n*) for each experimental group/condition, given as a discrete number and unit of measurement
☐	☒	A statement on whether measurements were taken from distinct samples or whether the same sample was measured repeatedly
☐	☒	The statistical test(s) used AND whether they are one- or two-sided *Only common tests should be described solely by name; describe more complex techniques in the Methods section.*
☒	☐	A description of all covariates tested
☐	☒	A description of any assumptions or corrections, such as tests of normality and adjustment for multiple comparisons
☐	☒	A full description of the statistical parameters including central tendency (e.g. means) or other basic estimates (e.g. regression coefficient) AND variation (e.g. standard deviation) or associated estimates of uncertainty (e.g. confidence intervals)
☐	☒	For null hypothesis testing, the test statistic (e.g. *F*, *t*, *r*) with confidence intervals, effect sizes, degrees of freedom and *P* value noted *Give P values as exact values whenever suitable.*
☒	☐	For Bayesian analysis, information on the choice of priors and Markov chain Monte Carlo settings
☒	☐	For hierarchical and complex designs, identification of the appropriate level for tests and full reporting of outcomes
☒	☐	Estimates of effect sizes (e.g. Cohen's *d*, Pearson's *r*), indicating how they were calculated

Our web collection on statistics for biologists contains articles on many of the points above.

Software and code

Policy information about availability of computer code

Data collection	Olymphus cellSens Standard 1.18 (for microscopic images), BD FACSDiva 8.0.1 10X chromium 5'-mRNA library and BCR library kit HISEQ4000 (illumina sequencing)
Data analysis	Graphpad Prism 7.0a & 8.0, FlowJo 10.4.2, Cell Ranger 2.2.0 (10X chromium), Rv3.4.2, Python 3.5.4, IgBlast v1.7.0, Seurat v2, Chage-O v0.4.2, Alakazam v0.2.11, PHYLIP 3.696

For manuscripts utilizing custom algorithms or software that are central to the research but not yet described in published literature, software must be made available to editors/reviewers. We strongly encourage code deposition in a community repository (e.g. GitHub). See the Nature Research guidelines for submitting code & software for further information.

Data

Policy information about availability of data

All manuscripts must include a data availability statement. This statement should provide the following information, where applicable:

- Accession codes, unique identifiers, or web links for publicly available datasets
- A list of figures that have associated raw data
- A description of any restrictions on data availability

RNA-seq data will be deposited and made public in the BioProject under accession number PRJNA524497.

Field-specific reporting

Please select the one below that is the best fit for your research. If you are not sure, read the appropriate sections before making your selection.

☒ Life sciences ☐ Behavioural & social sciences ☐ Ecological, evolutionary & environmental sciences

For a reference copy of the document with all sections, see nature.com/documents/nr-reporting-summary-flat.pdf

Life sciences study design

All studies must disclose on these points even when the disclosure is negative.

Sample size	No sample-size calculation was performed. We aimed to get at least 3 sample sizes in each group in each independent experiment based on our previous studies and/or pilot studies.
Data exclusions	No data were excluded.
Replication	Experiments were repeated with at least two biologically independent for all results presented in the manuscript. If the group size was small (due to limited availability of reagents or mouse strains), data from replicate experiments were pooled for graphical representation. All replicates are biological replicates obtained from biologically independent experiments.
Randomization	Allocation was not random. Since we used littermate animals in each experimental and control groups, randomization was not relevant to our study.
Blinding	All animal studies were not blinded since treatment and experimental analysis could not be separated, blinding of the investigators was not possible.

Reporting for specific materials, systems and methods

We require information from authors about some types of materials, experimental systems and methods used in many studies. Here, indicate whether each material, system or method listed is relevant to your study. If you are not sure if a list item applies to your research, read the appropriate section before selecting a response.

Materials & experimental systems

n/a	Involved in the study
☐	☒ Antibodies
☐	☒ Eukaryotic cell lines
☒	☐ Palaeontology
☐	☒ Animals and other organisms
☒	☐ Human research participants
☒	☐ Clinical data

Methods

n/a	Involved in the study
☒	☐ ChIP-seq
☐	☒ Flow cytometry
☒	☐ MRI-based neuroimaging

Antibodies

Antibodies used

antibody name/ supplier name /catalog number /clone name/ lot number /dilution /validation (website)
CD16/32 BioXCell BE0307 2.4G2 1:500 https://bxcell.com/product/invivomab-anti-mouse-cd16-cd32/
CD45.2 BioLegend 109824 104 B240422 1:300 https://www.biolegend.com/en-us/products/apc-cyanine7-anti-mouse-cd45-2-antibody-3906
CD45.1 BioLegend 110708 A20 B146359 1:300 https://www.biolegend.com/en-us/products/pe-anti-mouse-cd45-1-antibody-199
CD45 BioLegend 103116 30-F11 B266564 1:300 https://www.biolegend.com/en-us/products/apc-cyanine7-anti-mouse-cd45-antibody-2530
CD3e BioLegend 100308 145-2C11 B253780 1:300 https://www.biolegend.com/en-us/products/pe-anti-mouse-cd3epsilon-antibody-25
CD4 BioLegend 100451 GK1.5 B223832 1:300 https://www.biolegend.com/en-us/products/brilliant-violet-605-anti-mouse-cd4-antibody-10708
CD4 BioLegend 100540 RM4-5 B161056 1:300 https://www.biolegend.com/en-us/products/percpcyeanine5-5-anti-mouse-cd4-antibody-4230
CD8a BioLegend 100744 53-6.7 B266536 1:300 https://www.biolegend.com/en-us/products/brilliant-violet-605-anti-mouse-cd8a-antibody-7636
CD8a BioLegend 100747 53-6.7 B259952 1:300 https://www.biolegend.com/en-us/products/brilliant-violet-711-anti-mouse-cd8a-antibody-7926
CD19 BioLegend 115540 6D5 B264622 1:200 https://www.biolegend.com/en-us/products/brilliant-violet-605-anti-mouse-cd19-antibody-7645
CD19 BD Biosciences 564296 1D3 8039779 1:200 http://www.bdbiosciences.com/us/reagents/research/antibodies-buffers/immunology-reagents/anti-mouse-antibodies/cell-surface-antigens/buv737-rat-anti-mouse-cd19-1d3/p/564296

CD45R/B220 BioLegend 103236 RA3-6B2 B253647 1:200 https://www.biolegend.com/en-us/products/percp-cy5-5-anti-mouse-human-cd45r-b220-antibody-4267
CD138 BioLegend 142519 281-2 B248101 1:200 https://www.biolegend.com/en-us/products/brilliant-violet-711-anti-mouse-cd138-syndecan-1-antibody-8909
CD138 BioLegend 142507 281-2 B253736 1:200 https://www.biolegend.com/en-us/products/brilliant-violet-421-anti-mouse-cd138-syndecan-1-antibody-7852
CD38 BioLegend 102717 90 B242687 1:200 https://www.biolegend.com/en-us/products/pe-cy7-anti-mouse-cd38-antibody-3926
CD38 BioLegend 102719 90 B139813 1:200 https://www.biolegend.com/en-us/products/pacific-blue-anti-mouse-cd38-antibody-6652
GL7 BD Biosciences 561530 GL7 4330708 1:200 http://www.bdbiosciences.com/ds/pm/tds/561530.pdf
MHCII (I-A/I-E) BioLegend 107622 M5/114.15.2 B264454 1:800 https://www.biolegend.com/en-us/products/alexa-fluor-700-anti-mouse-i-a-i-e-antibody-3413
CD11c BioLegend 117329 N418 B258584 1:200 https://www.biolegend.com/en-us/products/brilliant-violet-421-anti-mouse-cd11c-antibody-7149
IgD BD Biosciences 564274 11-26c.2a 8046964 1:200 http://www.bdbiosciences.com/us/reagents/research/antibodies-buffers/second-step-reagents/anti-ig/buv395-rat-anti-mouse-igd-11-26c2a/p/564274
CD44 BioLegend 103026 IM7 B244378 1:200 https://www.biolegend.com/en-us/products/alexa-fluor-700-anti-mouse-human-cd44-antibody-3406
PD-L2 BioLegend 107210 TY25 B245340 1:200 https://www.biolegend.com/en-us/products/apc-anti-mouse-cd273-b7-dc--pd-l2-antibody-12353
CD80 BioLegend 104734 16-10A1 B249923 1:200 https://www.biolegend.com/en-us/products/pe-cy7-anti-mouse-cd80-antibody-9320
CD69 BioLegend 104512 H1.2F3 B253212 1:200 https://www.biolegend.com/en-us/products/pe-cy7-anti-mouse-cd69-antibody-3168
CD86 BioLegend 105011 GL1 B245161 1:200 https://www.biolegend.com/en-us/products/apc-anti-mouse-cd86-antibody-2896
AF488 goat anti-mouse IgG (H+L) Invitrogen A11029 polyclonal 1829910 1:800
AF647 donkey anti-mouse IgG (H+L) Fab Jackson ImmunoResearch 715-607-003 polyclonal 128907 1:600
CCR1 R&D Systems FAB5986P 643854 ABQH0314071 10ul/test https://www.rndsystems.com/products/mouse-ccr1-pe-conjugated-antibody-643854_fab5986p
CCR2 R&D Systems FAB5538F 475301 ABPZ0212011 10ul/test https://www.rndsystems.com/products/mouse-ccr2-fluorescein-conjugated-antibody-475301_fab5538f
CCR3 BD Biosciences 557974 83103 1:200 http://www.bdbiosciences.com/us/applications/research/t-cell-immunology/th-2-cells/surface-markers/mouse/alexa-fluor-647-rat-anti-mouse-cd193-83103/p/557974
CCR4 BioLegend 131214 2G12 B201546 1:200 https://www.biolegend.com/en-us/products/pe-cy7-anti-mouse-cd194-ccr4-antibody-6333
CCR5 BioLegend 107012 HM-CCR5 B186964 1:200 https://www.biolegend.com/en-us/products/apc-anti-mouse-cd195-ccr5-antibody-3939
CCR6 BioLegend 129815 29-2L17 B187956 1:200 https://www.biolegend.com/en-us/products/pe-cy7-anti-mouse-cd196-ccr6-antibody-6152
CCR7 BioLegend 120105 4B12 B254167 1:200 https://www.biolegend.com/en-us/products/pe-anti-mouse-cd197-ccr7-antibody-2799
CCR8 BioLegend 150311 SA214G2 B224699 1:200 https://www.biolegend.com/en-us/products/pe-anti-mouse-cd198-ccr8-antibody-13428
CCR9 BioLegend 128705 CW-1.2 B120356 1:200 https://www.biolegend.com/en-us/products/fitc-anti-mouse-cd199-ccr9-antibody-5123
CCR10 R&D Systems FAB2815P 248918 LXL0207011 10ul/test https://www.rndsystems.com/products/mouse-ccr10-pe-conjugated-antibody-248918_fab2815p
CXCR1 R&D Systems FAB8628P 1122A AENE0115111 10ul/test https://www.rndsystems.com/products/mouse-cxcr1-il-8-ra-pe-conjugated-antibody-1122a_fab8628p
CXCR2 BioLegend 129101 TG11/CXCR2 B119951 1:200
CXCR3 BioLegend 126506 CXCR3-173 B137934 1:200 https://www.biolegend.com/en-us/products/pe-anti-mouse-cd183-cxcr3-antibody-4592
CXCR3 BioLegend 126512 CXCR3-173 B233225 1:200 https://www.biolegend.com/en-us/products/apc-anti-mouse-cd183-cxcr3-antibody-4683
CXCR4 BD Biosciences 551966 2B11/CXCR4 1:200 http://www.bdbiosciences.com/us/applications/research/t-cell-immunology/regulatory-t-cells/surface-markers/mouse/pe-rat-anti-mouse-cd184-2b11cxcr4/p/551966
CXCR5 BioLegend 145515 L138D7 B170134 1:200 https://www.biolegend.com/en-us/products/pe-cy7-anti-mouse-cd185-cxcr5-antibody-8617
CXCR6 BioLegend 151105 SA051D1 B224895 1:200 https://www.biolegend.com/en-us/products/apc-anti-mouse-cd186-cxcr6-antibody-13065
IFN-g BioLegend 505810 XMG1.2 B221722 1:200 https://www.biolegend.com/en-us/products/apc-anti-mouse-ifn-gamma-antibody-993
CD4 blocking Ab BioXCell BE0003-1 GK1.5 699918M2 https://bxcell.com/product/m-cd4/
IFN-g blocking Ab BioXCell BE0054 R4-6A2 601516A2 https://bxcell.com/product/m-inf-gamma/
FITC mouse IgG Jackson ImmunoResearch 211-095-109 polyclonal 131785
mIgG1 anti-HSV gD MAb Absolute Antibody Ab00442-1.1 E317 T1832B15 https://absoluteantibody.com/product/anti-glycoprotein-d-of-hsv-e317/Ab00442-1.1_Mouse_IgG1/
CD4 BD Biosciences 553649 H129.19 1:320 http://www.bdbiosciences.com/us/applications/research/t-cell-immunology/th-1-cells/surface-markers/mouse/biotin-rat-anti-mouse-cd4-h12919/p/553649
CD45R/B220 BioLegend 103208 RA3-6B2 B224683 1:200 https://www.biolegend.com/en-us/products/pe-anti-mouse-human-cd45r-b220-antibody-447
CD138 BioLegend 142511 281-2 B183667 1:100 https://www.biolegend.com/en-us/products/biotin-anti-mouse-cd138-syndecan-1-antibody-8449
CD31 eBioscience 13-0311-81 390 1:100 https://www.thermofisher.com/antibody/product/CD31-PECAM-1-Antibody-clone-390-Monoclonal/13-0311-81

VCAM-1 BioLegend 105703 429/MVCAM.A 1:100 https://www.biolegend.com/en-us/products/biotin-anti-mouse-cd106-antibody-136
AF647 anti-FITC Ab Jackson ImmunoResearch 200-602-037 135650
AF568 anti-mouse IgG (H+L) Invitrogen A10037 polyclonal
FITC pAbs against HSV1 and 2 Virostat 0196
HRP-conjugated anti-mouse IgG1 SouthernBiotech 1070-05 polyclonal D0812-WC82B 1:1000 https://www.southernbiotech.com/?catno=1070-05&type=Polyclonal#&panel1-1&panel2-1
HRP-conjugated anti-mouse IgG3 SouthernBiotech 1100-05 polyclonal B0308-Z781C 1:1000 https://www.southernbiotech.com/?catno=1100-05&type=Polyclonal#&panel1-1&panel2-1
HRP-conjugated anti-mouse IgM SouthernBiotech 1020-05 polyclonal C0012-P252L 1:1000 https://www.southernbiotech.com/?catno=1020-05&type=Polyclonal#&panel2-1
HRP-conjugated anti-mouse IgA SouthernBiotech 1040-05 polyclonal I5613-R566B 1:1000 https://www.southernbiotech.com/?catno=1040-05&type=Polyclonal#&panel1-1&panel2-1
HRP-conjugated anti-mouse IgG2b SouthernBiotech 1090-05 polyclonal A2513-XA54E 1:1000 https://www.southernbiotech.com/?catno=1090-05&type=Polyclonal#&panel1-1&panel2-1
HRP-conjugated anti-mouse IgG2c SouthernBiotech 1079-05 polyclonal G0313-ZF85D 1:1000 https://www.southernbiotech.com/?catno=1079-05&type=Polyclonal#&panel2-1

Validation

Quality of antibodies was tested by manufacturer (statements on the manufacturer's website) or relevant references were cited on the manufacturer's website. Vendor websites for antibodies were listed above and the validations can be found there.

Eukaryotic cell lines

Policy information about cell lines

Cell line source(s)

Vero cells (ATCC CCL-81)

Authentication

Cell lines were authenticated by morphology.

Mycoplasma contamination

Cell lines were routinely tested for mycoplasma contamination, and negative for mycoplasma contamination.

Commonly misidentified lines
(See ICLAC register)

No misidentified cell lines in this study

Animals and other organisms

Policy information about studies involving animals; ARRIVE guidelines recommended for reporting animal research

Laboratory animals

Six to eight-week old female C57BL/6 (CD45.2+), congenic C57BL/6 B6.SJL-PtprcaPep3b/BoyJ (B6.Ly5.1) (CD45.1+), B6.129S2-IghtmlCgn/J (μMT), B6.FVB-Tg[ITGAM-DTR/EGFP] 34Lan/J (CD11bDTR), B6.Cg-Tg(CAG-DsRed*MST)1Nagy/J (DsRed), and B6.129P2-Cxcr3tm1Dgen/J (CXCR3-/-) mice from the National Cancer Institute and Jackson Laboratory

Wild animals

No wild animals were used in this study

Field-collected samples

No field-collected samples were used in this study

Ethics oversight

All procedures used in this study complied with federal guidelines and institutional policies by the Yale animal care and use committee (Protocol # 2018-10365).

Note that full information on the approval of the study protocol must also be provided in the manuscript.

Flow Cytometry

Plots

Confirm that:

☐ The axis labels state the marker and fluorochrome used (e.g. CD4-FITC).

☒ The axis scales are clearly visible. Include numbers along axes only for bottom left plot of group (a 'group' is an analysis of identical markers).

☐ All plots are contour plots with outliers or pseudocolor plots.

☒ A numerical value for number of cells or percentage (with statistics) is provided.

Methodology

Sample preparation

The genital tracts of vaginal tissues and upper reproductive tracts including cervix and uterus treated with Depo-Provera were dissected from the urethra and cervix. Tissues were then incubated with 0.5 mg/mL Dispase II (Roche) for 15 min at 37 °C. Thereafter, tissues were digested with 1 mg/mL collagenase D (Roche) and 30 μg/mL DNase I (Sigma-Aldrich) at 37 °C for 25 min. The resulting cells were filtered through a 70-μm filter and single cells were isolated.

Instrument

LSRII flow cytometer

Software	FACS DIVA, FlowJo 10.4.2
Cell population abundance	For B cell-sorted spleen samples, cell numbers were counted and 6,000 cells were prepared. Cells from primary and secondary infected FRT samples were prepared at a cell count proportional to the immune cell infiltration observed by flow cytometry. We separate CD3 and CD19 expressing clusters during scRNA seq analysis.
Gating strategy	live/dead stain (Aqua)- gated -> CD45.2+ or CD45.1+ gated -> single cells (FSC-A/FSC-H) -> lymphocytes gated. We defined positive and negative population at the distinct border or by using isotype control stain.

☐ Tick this box to confirm that a figure exemplifying the gating strategy is provided in the Supplementary Information.